NATIONAL ENERGY TECHNOLOGY LABORATORY

Characterization of the Martinsburg Formation using Computed Tomography and Geophysical Logging Techniques

2 March 2017

U.S. DEPARTMENT OF ENERGY | NATIONAL ENERGY TECHNOLOGY LABORATORY

Office of Fossil Energy

NETL-TRS-4-2017

Disclaimer

This report was prepared as an account of work sponsored by an agency of the United States Government. Neither the United States Government nor any agency thereof, nor any of their employees, makes any warranty, express or implied, or assumes any legal liability or responsibility for the accuracy, completeness, or usefulness of any information, apparatus, product, or process disclosed, or represents that its use would not infringe privately owned rights. Reference therein to any specific commercial product, process, or service by trade name, trademark, manufacturer, or otherwise does not necessarily constitute or imply its endorsement, recommendation, or favoring by the United States Government or any agency thereof. The views and opinions of authors expressed therein do not necessarily state or reflect those of the United States Government or any agency thereof.

Cover Illustration: The upper most circle represents images taken of samples analyzed in this report. The left most circle represents the multi-sensor core logger in diagram format with associated pictures of the instrument in operation and the final data product (bottom). The right most circle shows pictures of the medical (top) and industrial (bottom) computed tomography units, with the images to the left and right being products from the analysis contained within this report.

Suggested Citation: Crandall, D.; Moore, J.; Rodriguez, R.; Gill, M.; Soeder, D.; McIntyre, D.; Brown, S. *Characterization of Martinsburg Formation using Computed Tomography and Geophysical Logging Techniques;* NETL-TRS-4-2017; NETL Technical Report Series; U.S. Department of Energy, National Energy Technology Laboratory: Morgantown, WV, 2017; p 68.

An electronic version of this report can be found at:

http://netl.doe.gov/research/on-site-research/publications/featured-technical-reports

https://edx.netl.doe.gov/ucr

The data in this report can be accessed from NETL's Energy Data eXchange (EDX) online system (https://edx.netl.doe.gov) using the following link: https://edx.netl.doe.gov/dataset/martinsburg-formation-ct-data

Characterization of the Martinsburg Formation using Computed Tomography and Geophysical Logging Techniques

Dustin Crandall[1,2], Johnathan Moore[2,3], Rebecca Rodriguez[3], Magdalena Gill[2], Daniel Soeder[1], Dustin McIntyre[1], Sarah Brown[2]

[1] U.S. Department of Energy, Office of Research and Development, National Energy Technology Laboratory, 3610 Collins Ferry Road, Morgantown, WV 26507

[2] U.S. Department of Energy, AECOM, National Energy Technology Laboratory, 3610 Collins Ferry Road, Morgantown, WV 26507

[3] U.S. Department of Energy, ORAU, National Energy Technology Laboratory, 3610 Collins Ferry Road, Morgantown, WV 26507

NETL-TRS-4-2017

2 March 2017

NETL Contacts:

Dustin Crandall, Principal Investigator

J. Alexandra Hakala, Technical Portfolio Lead

Cynthia Powell, Executive Director, Research & Innovation Center

This page intentionally left blank.

Table of Contents

ABSTRACT **1**
1. INTRODUCTION **2**
2. GEOLOGY AND SITE OVERVIEW **6**
3. DATA ACQUISITION AND METHODOLOGY **8**
3.1 CORE LOGGING 8
3.2 MEDICAL CT SCANNING 10
3.3 GEOLOGIC EVALUATION 12
3.4 DATA COMPILATION 12
3.5 INDUSTRIAL CT 12
4. RESULTS **16**
5. DISCUSSION **57**
6. REFERENCES **59**

List of Figures

Figure 1: Lost River Dam location in Hardy County West Virginia, shown by red dot. 3
Figure 2: Correlation chart of Middle Proterozoic, Cambrian, and Ordovician rocks along section D-D' 4
Figure 3: Initial diagrams for construction of the Lost Creek watershed dam site. 5
Figure 4: Surface topologic map of Lost River Dam location. 6
Figure 5: Representation of generalized MSCL with all attached instruments. 8
Figure 6: Periodic table showing elements measurable by the Innov-X® X-Ray Fluorescence Spectrometer 10
Figure 7: Toshiba® Aquilion™ Multislice Helical Computed Tomography Scanner at the NETL used for core analysis. 11
Figure 8: Medical CT scans of Lost River core from Drill Hole #254 from a depth of 31.9 to 40.1 ft. 11
Figure 9: Core samples as received in boxes with place-holders for missing section. 12
Figure 10: Side view (A) and top view down (B) of rotation inconsistencies with industrial scanner and objects longer than 2 in. that require multiple scans. 14
Figure 11: Lost River core Drill Hole #51, medical CT scans from 20.0 to 33.7 ft. 17
Figure 12: Lost River core Drill Hole #51, medical CT scans from 33.9 to 42.0 ft. 18
Figure 13: Lost River core Drill Hole #51, medical CT scans from 42.4 to 47.0 ft. 19
Figure 14: Lost River core Drill Hole #61, medical CT scans from 25.2 to 35.8 ft. 20
Figure 15: Lost River core Drill Hole #61, medical CT scans from 35.8 to 50.0 ft. 21
Figure 16: Lost River core Drill Hole #251, medical CT scans from 40.0 to 50.0 ft. 22
Figure 17: Lost River core Drill Hole #252, medical CT scans from 31.0 to 51.0 ft. 23
Figure 18: Lost River core Drill Hole #254, medical CT scans from 28.0 to 43.0 ft. 24
Figure 19: Lost River core Drill Hole #254, medical CT scans from 43.0 to 58.2 ft. 25
Figure 20: Lost River core Drill Hole #254, medical CT scans from 58.2 to 72.0 ft. 26
Figure 21: Lost River core Drill Hole #254, medical CT scans from 72.0 to 87.0 ft. 27
Figure 22: Lost River core Drill Hole #254, medical CT scans from 87.0 to 100.0 ft. 28
Figure 23: Lost River core Drill Hole #255, medical CT scans from 16.0 to 25.6 ft. 29
Figure 24: Lost River core Drill Hole #255, medical CT scans from 25.6 to 35.4 ft. 30
Figure 25: Lost River core Drill Hole #255, medical CT scans from 35.4 to 44.9 ft. 31
Figure 26: Lost River core Drill Hole #256, medical CT scans from 18.0 to 29.1 ft. 32
Figure 27: Lost River core Drill Hole #256, medical CT scans from 29.1 to 39.9 ft. 33
Figure 28: Lost River core Drill Hole #256, medical CT scans from 39.9 to 49.2 ft. 34
Figure 29: Lost River core Drill Hole #256, medical CT scans from 49.2 to 60.0 ft. 35
Figure 30: Lost River core Drill Hole #256, medical CT scans from 60.0 to 70.5 ft. 36
Figure 31: Lost River core Drill Hole #651, medical CT scans from 10.0–19.6 ft. 37
Figure 32: Lost River core Drill Hole #651, medical CT scans from 19.6–31.7 ft.. 38
Figure 33: Lost River core Drill Hole #651, medical CT scans from 31.7–40.0 ft.. 39
Figure 34: Lost River core Drill Hole #751, medical CT scans from 11.5–23.8 ft. 40
Figure 35: Lost River core Drill Hole #751, medical CT scans from 24.4–33.0 ft. 41
Figure 36: Lost River core Drill Hole #751, medical CT scans from 33.0 to 42.0 ft.. 42
Figure 37: Combined core log for Lost River 27 Drill Hole #51. 44
Figure 38: Combined core log for Lost River 27 Drill Hole #61. 45
Figure 39: Combined core log for Lost River 27 Drill Hole #251. 46

List of Figures (cont.)

Figure 40: Combined core log for Lost River 27 Drill Hole #252. 47
Figure 41: Combined core log for Lost River 27 Drill Hole #254. 48
Figure 42: Combined core log for Lost River 27 Drill Hole #255. 49
Figure 43: Combined core log for Lost River 27 Drill Hole #256. 50
Figure 44: Combined core log for Lost River 27 Drill Hole #651. 51
Figure 45: Combined core log for Lost River 27 Drill Hole #751. 52
Figure 46: 3D representation of features from Lost River Drill Hole #251 at depth 40.2–41 feet. 54
Figure 47: 3D representation of features from Lost River Drill Hole #254 at depth 72.9–73.5 feet. 55
Figure 48: 3D representation of features from Lost River Drill Hole #751 at depth 36.0–36.4 feet. 56

List of Tables

Table 1: Magnetic Susceptibility values for common minerals..... 9

Acronyms, Abbreviations, and Symbols

Term	Description
2D	Two -dimensional
3D	Three-dimensional
CT	Computed tomography
MSCL	Multi-Sensor Core Logger
RIC	Research & Innovation Center
WVGES	West Virginia Geologic and Economic Survey
XRF	X-ray fluorescence

Acknowledgments

This work was completed as part of National Energy Technology Laboratory (NETL) research for the U.S. Department of Energy's (DOE) Complementary Research Program under Section 999 of the Energy Policy Act of 2005. The authors wish to acknowledge Ray Boswell (NETL Strategic Center for Natural Gas and Oil) and Elena Melchert (DOE Office of Fossil Energy) for programmatic guidance, direction, and support.

The authors would like to thank Bryan Tennant, Karl Jarvis and Roger Lapeer for making the CT scanner lab functional. Thank you to the West Virginia Geologic Survey for allowing us to work with this core. This research was supported in part by appointments from the NETL Research Participation Program, sponsored by the U.S. DOE and administered by the Oak Ridge Institute for Science and Education.

This page intentionally left blank.

ABSTRACT

The computed tomography (CT) facilities and the Multi-Sensor Core Logger (MSCL) at the National Energy Technology Laboratory (NETL) Morgantown site were used to characterize 9 different core sections of Upper Ordovician black shale from the Eastern Panhandle of West Virginia. The samples are representative of the upper Ordovician Martinsburg Formation, a Utica Shale equivalent, which is a carbonaceous black shale in the Appalachian Basin. The primary impetus of this work was to develop a standardized methodology for the rapid and detailed characterization of chemical composition, physical characteristics, and internal micro structure of lithologic samples with the NETL core characterization equipment. Having a standardized methodology combining these innovative techniques allows large, rapidly produced data sets to be available for multiple researchers and allows collaborative studies. The resultant data sets are presented as part of this report as well and can be accessed from NETL's Energy Data eXchange (EDX) online system (https://edx.netl.doe.gov) using the following link: https://edx.netl.doe.gov/dataset/martinsburg-formation-ct-data.

All equipment and techniques used were non-destructive, enabling future examinations to be performed on these cores with the additional information gathered through these tests. None of the equipment used was suitable for direct visualization of the shale pore space, though fractures and discontinuities were visible and detectable with all methods tested. High resolution CT imagery with the NETL industrial CT scanner was a powerful and insightful way to examine the details of fractures, discontinuities, minerals, and large crystals within the shale, but was time consuming both in image capture and analysis. As such, only a small percentage of the core was scanned at high resolution. Low resolution CT imagery with the NETL medical CT scanner was performed on the entire core. Qualitative analysis of the medical CT images, coupled with the measurements from the multi-sensor core logger (including x-ray fluorescence, XRF, measurements) were very useful in identifying zones of interest for more detailed analysis and fractured zones. The ability to quickly identify key areas for more detailed study with higher resolution will save time and resources in future studies. The combination of all methods used provided a multi-scale analysis of this core and provided both a macro and micro description of the core that is relevant for many subsurface energy related examinations of core that have traditionally been performed at NETL.

1. INTRODUCTION

Evaluation of reservoir samples prior to production for resource estimation and effective extraction methodology is critical in the development of subsurface resources. While it is common for commercial entities to perform these characterizations, the resources necessary to conduct this analysis are not always available to the broader interest base, such as state surveys and research based consortiums. In order to meet the growing need for comprehensive and high quality lithologic data for collaborative research initiatives, NETL has used available resources in conjunction with previous techniques and new, innovative methodologies to develop a systematic approach for the evaluation of lithologic samples. In this report, the data collection techniques and preliminary analysis of the Martinsburg shale are presented to highlight the methodologies and capabilities of the Research & Innovation Center (RIC) researchers at National Energy Technology Laboratory (NETL) and how this new procedure will help streamline the data produced.

In this study the primary objective was to develop a standardized methodology and techniques for analysis of core samples in order to have processes developed for future core analysis and to provide planning guidance to entities wishing to utilize NETL's characterization expertise. The data is presented in several formats that are potentially useful for various analyses, but little detailed analysis is presented in this report as the research objective was not to do a site characterization, but rather to develop the appropriate techniques to obtain data in a consistent fashion for site or regional characterizations.

The samples were acquired through a joint venture with the West Virginia Geologic Survey (WVGS). Nine (9) core samples were originally obtained as part of a geotechnical survey for a proposed earthen dam in the Lost River watershed in Hardy County, WV (Figures 1–3). Core sections ranged from 27 to 72 ft long, with varying degrees of recovery; in some instances up to 10 ft of consecutive core is missing. The sections that were fissile or had low recovery rates were not evaluated for the purposes of this study.

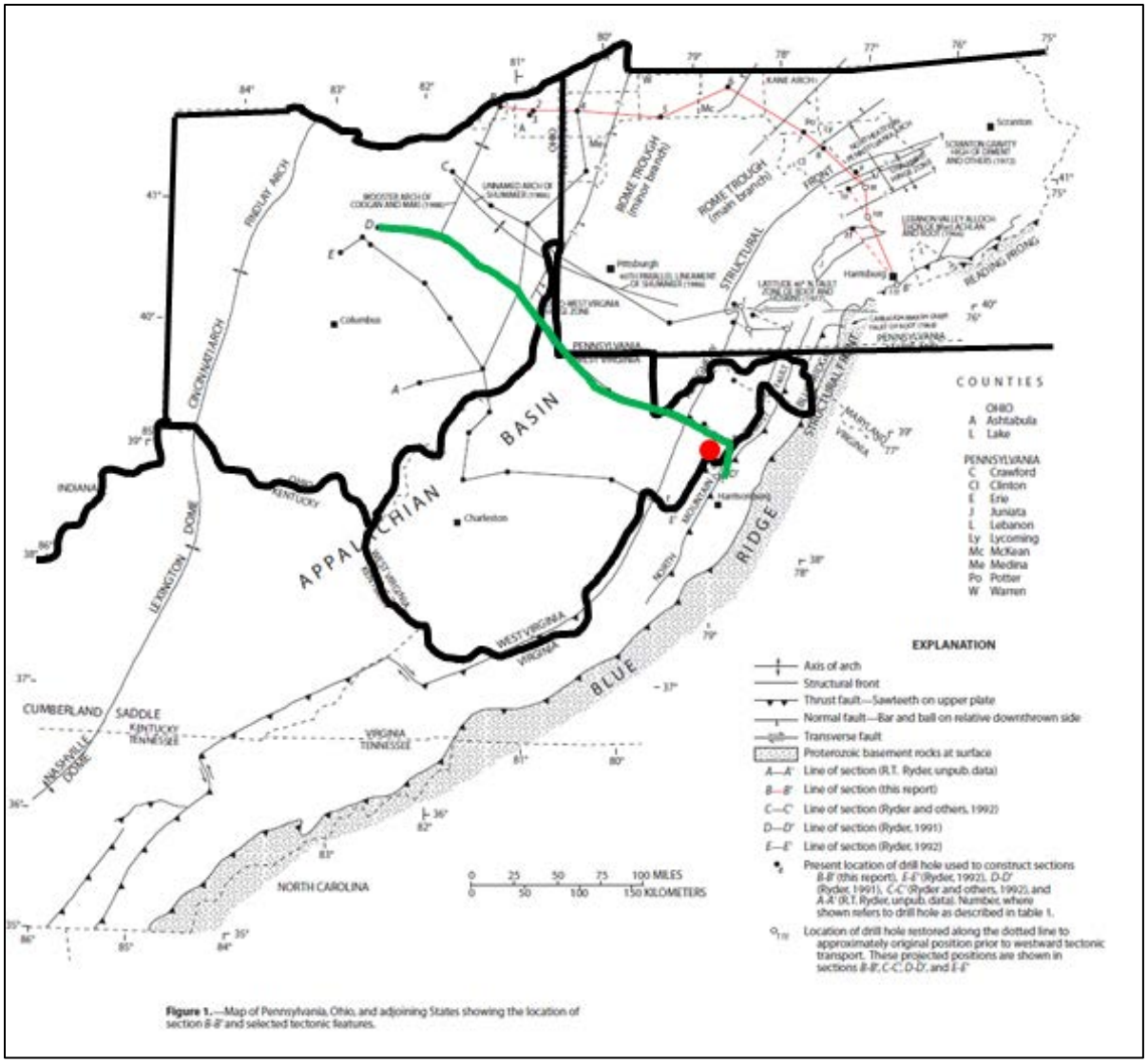

Figure 1.—Map of Pennsylvania, Ohio, and adjoining States showing the location of section B-B' and selected tectonic features.

Figure 1: Lost River Dam location in Hardy County West Virginia, shown by red dot.

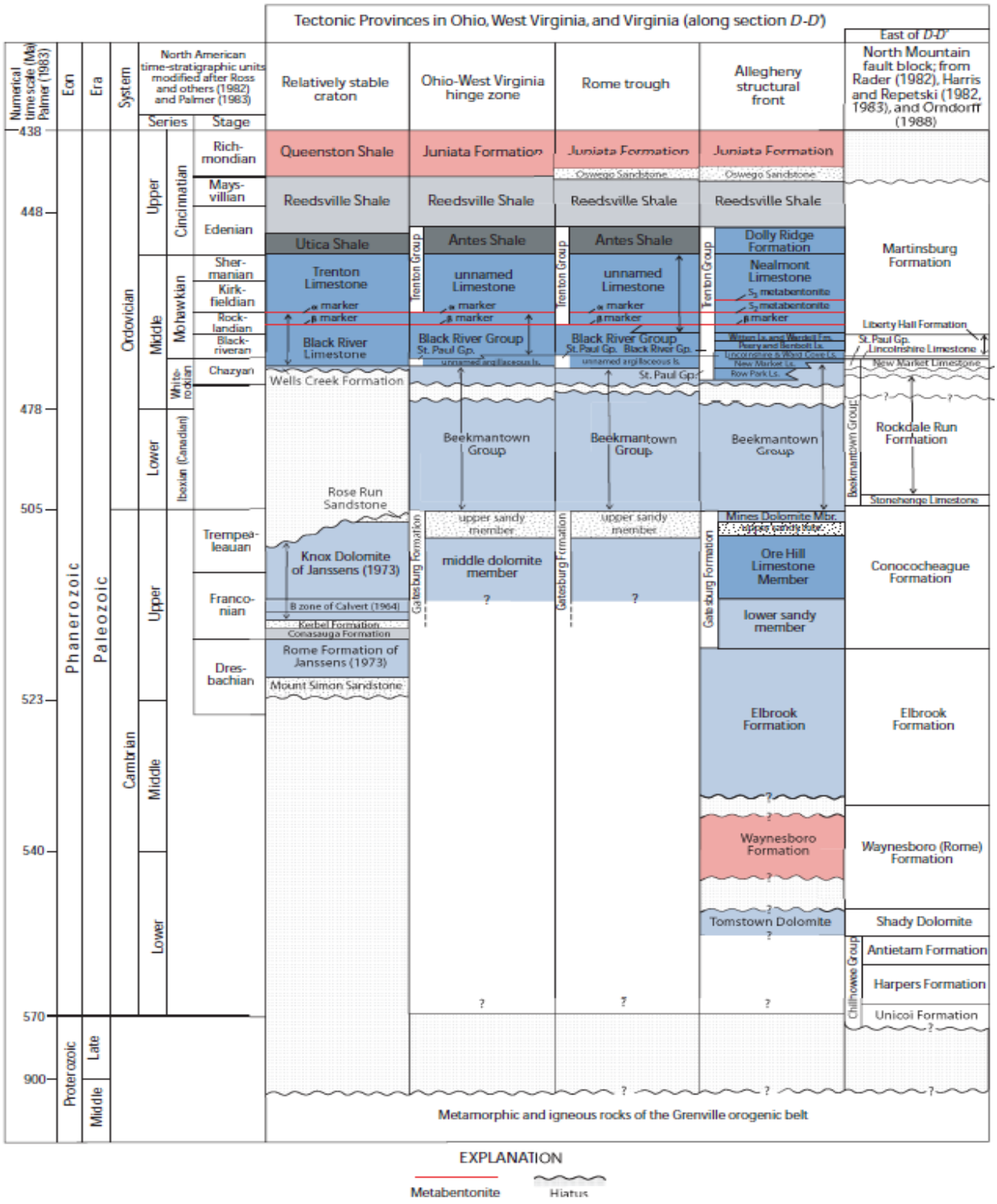

Figure 2: Correlation chart of Middle Proterozoic, Cambrian, and Ordovician rocks along section D-D' (solid green line) (Modified figures from Ryder and Crangle, 2002).

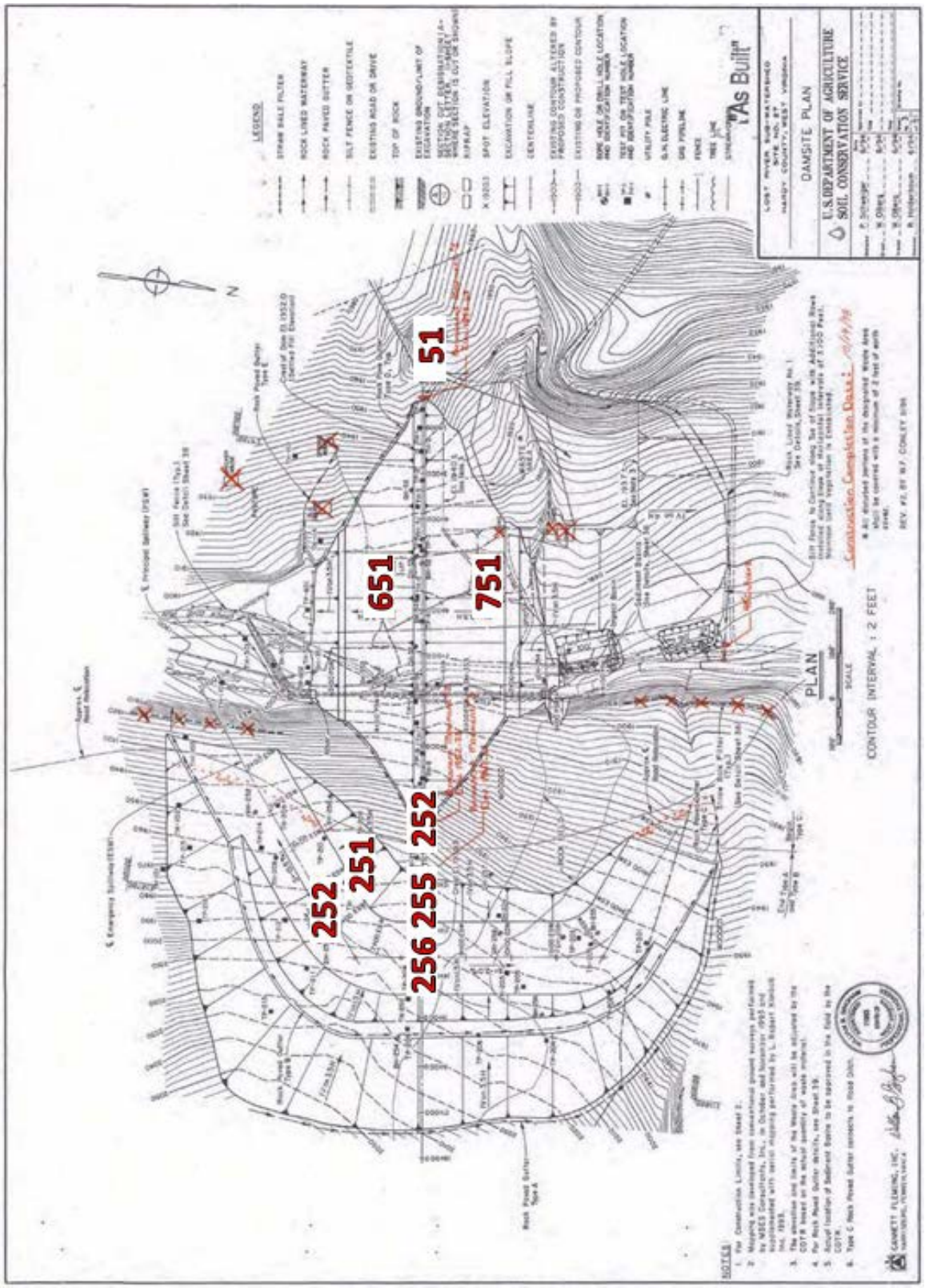

Figure 3: Initial diagrams for construction of the Lost Creek watershed dam site. Borehole locations marked in black.

2. GEOLOGY AND SITE OVERVIEW

The geologic unit immediately underlying the Lost Creek watershed dam location is the Martinsburg Group (Figures 1 and 2), which, in its lower limits, is a gray to black calcareous shale that is an equivalent of the Ordovician Utica Shale. Thin limestone and sandstone interbeds are scattered throughout the formation. Additionally, the lower intervals of the formation are fossiliferous and in some intervals highly fractured; fluid pathways are present along slickensides and cross bedding which have provided avenues for groundwater infiltration and mineral precipitation.

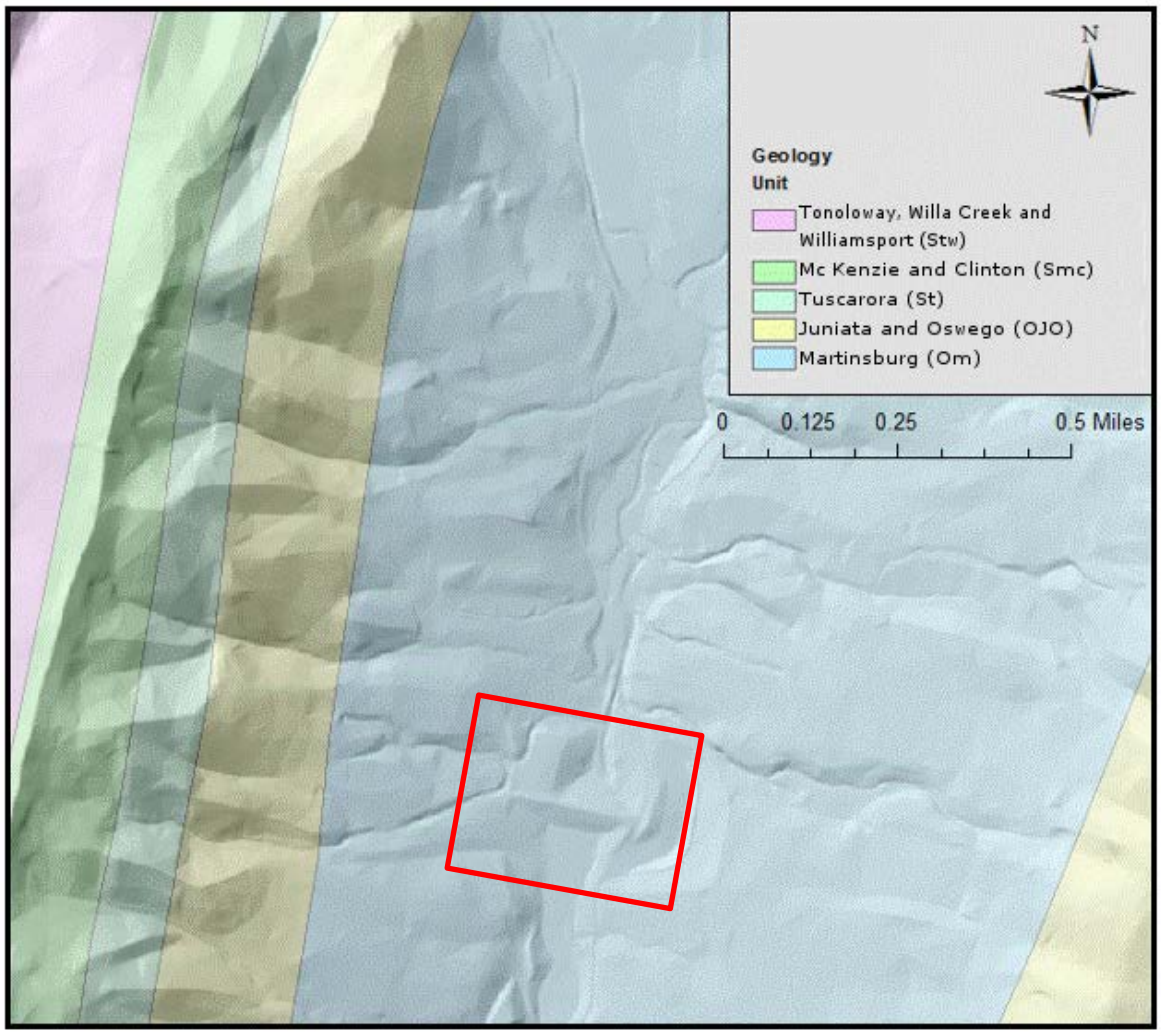

Figure 4: Surface topologic map of Lost River Dam location. Map is accentuated by underlying topography and the dam is readily visible in the center of the red box that outlines the area of the original survey from Figure 3.

The sample area resides on an anticlinal axis that controls the regional topography and geological structure (Figure 4). The Martinsburg Formation is thinnest near the axis of the anticline and thus closest to the base of the unit, indicating that this study is indeed examining samples from the

lower Martinsburg. An important note is that the lithologic units adjacent to the Martinsburg Fm are comprised primarily of weather-resistant, ridge-forming sandstones and carbonates, making the location ideal for dam installation.

3. DATA ACQUISITION AND METHODOLOGY

The samples were evaluated using various methodologies, including computed tomography (CT) scanning, geophysical and geochemical core logging, and hand-evaluation by geologists. All 9 cores were characterized in their entirety using the same protocols. Industrial CT scans, because of their time-consuming nature, were selectively conducted over regions of interest rather than the whole core.

3.1 CORE LOGGING

Geophysical measurements of core thickness deviation, P-wave travel time, P-wave signal amplitude, magnetic susceptibility, and attenuated gamma counts were obtained with a Geotek® Multi-Sensor Core Logging (MSCL) system. Geotek® MSCL software was used to process the raw data into core thickness, P-wave velocity, gamma density, and fractional porosity values. Additionally, the system was used to measure bulk elemental chemistry with a built-in, portable X-ray fluorescence (XRF) spectrometer. The Geotek® MSCL system at the NETL has many capabilities but only those that were significant to this characterization are described in the following sections (Figure 5).

3.1.1 P-Wave Velocity

P-Wave velocity measurements are performed to measure the acoustic impedance of a geologic sample with compressional waves. Impedance, in this setting, is a measure of how well a material transmits vibrations, which is directly proportional to density and/or material consolidation. An example of a material that has a high acoustic impedance would be air, with a wave speed of 330 m/s, whereas granite would have low acoustic impedance, with a wave speed of >5,000 m/s. The importance of these particular measurements is that they can be proxies for seismic reflection coefficients, and can be translated to field use when doing seismic surveys.

The software associated with the MSCL can measure the travel time of the pulse with a resolution of 50 ns. The absolute accuracy of the instrument measurements is ± 3 m/s with a resolution of 1.5 m/s (Geotek Ltd. Multi-Sensor Core Logger Manual, Version 05-10; Geotek Ltd., 2010).

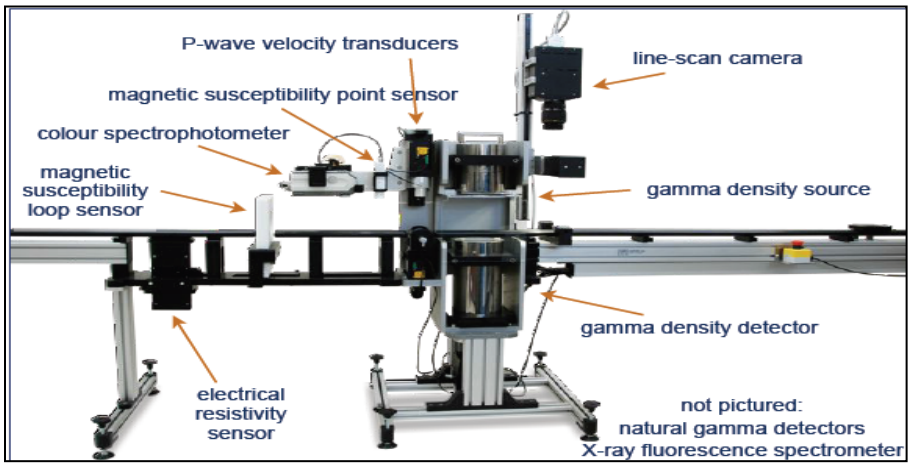

Figure 5: Representation of generalized MSCL with all attached instruments. From Geotek Ltd., Geotek Multi-Sensor Core Logger Flyer, Daventry, UK (2009).

3.1.2 Magnetic Susceptibility

Magnetic susceptibility is a measure of the degree of magnetization in the sample. The sample is passed through a ring apparatus with an oscillating magnetic field, where the interference to this field is proportional to the magnetism of the sample, and thus a relative measurement can be taken. The measurement unit used is dimensionless (abbreviated simply as SI units) and is based on the original calibration, which is done via stable iron oxides, and reference minerals which have known ranges of susceptibility (Table 1) (Geotek Ltd. Multi-Sensor Core Logger Manual, Version 05-10).

Table 1: Magnetic susceptibility values for common minerals (Modified from Geotek Ltd. Multi-Sensor Core Logger Manual, Version 05-10)

Mineral	X (*10^{-6}) SI
Water	9
Calcite	-7.5 to -39
Halite, Gypsum	-10 to -60
Illite, Montmorillonite	330 to 410
Pyrite	5 to 3,500
Haematite	500 to 40,000
Magnetite	1,000,000 to 5,700,000

3.1.3 Gamma Density

Gamma density is acquired by subjecting the sample to gamma radiation and then measuring the attenuation of that radiation. The attenuation is directly proportional to the density of the sample and is acquired by measuring the difference between radiation energy at the emission source and after it passes through the sample. Specifically, the MSCL software calculates the bulk density, ρ, by using the following equation:

$$\rho = \left(\frac{1}{\mu d}\right) \ln\left(\frac{I_o}{I}\right)$$

Where μ = Compton attenuation coefficient, d = thickness, I_o = source intensity, and I = measured intensity.

3.1.4 X-ray Fluorescence Spectrometry

In addition to the geophysical measurements a portable handheld Innov-X® X-Ray Fluorescence Spectrometer was used to measure relative elemental abundances of aggregated “light elements” up to and including sodium, and also various heavy elements which were measured individually (Figure 5). Elemental abundances are reported relative to the total elemental composition, i.e. out of 100% weight.

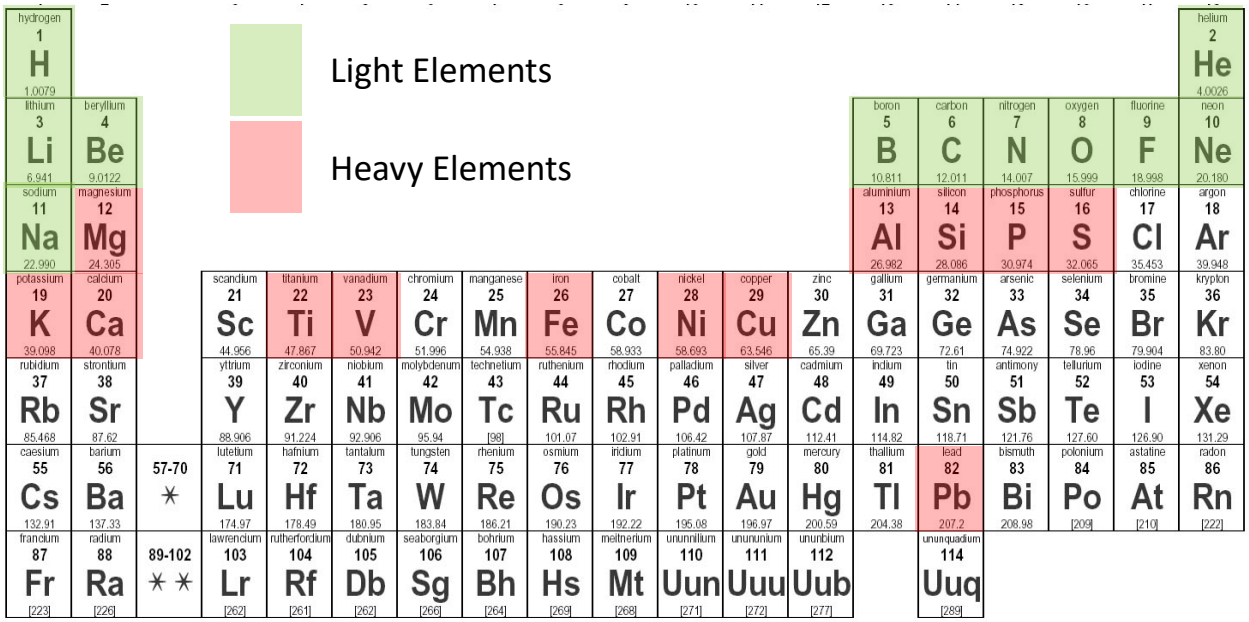

Figure 6: Periodic table showing elements measurable by the Innov-X® X-Ray Fluorescence Spectrometer

The XRF spectrometer measures elemental abundances by subjecting the sample to X-ray photons. The high energy of the photons displaces inner orbital electrons in the respective elements. The vacancies in the lower orbitals cause outer orbital electrons to "fall" into lower orbits to satisfy the disturbed electron configuration. The substitution into lower orbitals causes a release of a secondary X-ray photon, which has an energy associated with a specific element. These relative and element specific energy emissions can then be used to determine bulk elemental composition.

3.2 MEDICAL CT SCANNING

Core scale CT scanning was done with a medical Toshiba® Aquilion RXL™ Multislice Helical Computed Tomography Scanner (medical CT) as shown in Figure 7. The medical CT scanner generates images with a resolution in the millimeter range, with scans having voxel resolutions of 0.35 x 0.35 mm in the XY plane and 0.50 mm along the core axis. All scans were done in 3 foot or smaller sections, which resulted in image stacks of more than 1400 XY slices. The scans were conducted at a voltage of 80 kV and at 200 mA. Subsequent processing and combining of stacks was performed to create 3D volumetric representations of the cores and a 2D cross-section through the middle of the core samples. Examples of the processed output from this CT scanner are shown in Figure 8 for four sections of the Lost River site, Drill Hole #254, from a depth of 31.9 to 40.1 ft. The variation in greyscale values observed in the CT images indicates changes in the CT number obtained from the CT scans, which is directly proportional to changes in the attenuation and density of the scanned rock. Darker regions are less dense. As can be seen in Figure 8, filled fractures, open fractures, and changes in bedding structure can all be resolved via careful examination of the CT images. While the medical CT scanner was not used for detailed

characterization in this study, it allowed for non-destructive bulk characterization of all 9 core sections in their entirety, and thus complimented the MSCL data on the resultant logs.

Figure 7: Toshiba® Aquilion™ Multislice Helical Computed Tomography Scanner at the NETL used for core analysis.

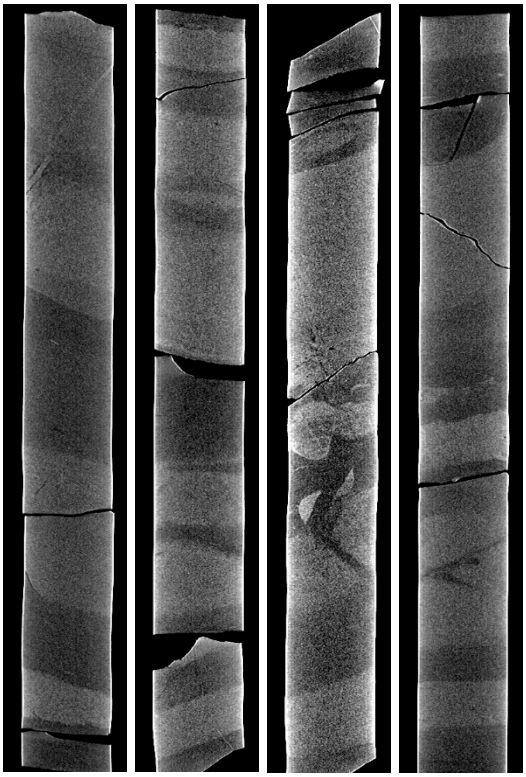

Figure 8: Medical CT scans of Lost River core from Drill Hole #254 from a depth of 31.9 to 40.1 ft.

3.3 GEOLOGIC EVALUATION

The core samples were evaluated using the methodologies developed by the Eastern Gas Shales Project (Dyman, 1981). As such, all core sections were evaluated and described using the Wentworth Grade Scale (Pettijohn, 1957), Bedding Terminology (Dunbar & Rogers, 1957), and Quantitative Terms Used in Describing Layered Rocks (Mckee and Weir, 1953). Core samples were left as is in the sample boxes and only disturbed when active evaluation was performed (Figure 9). While these methods were strictly adhered to, some variability does inherently exist in these evaluations due to the subjective nature of the analysis. The premise of using these tools and terminology was to maintain consistency, adhere to industry standards, and provide in-depth geologic descriptions to supplement and corroborate past and future analyses.

Standard tools and methods were used to examine the cores to determine the above characteristics. Grain size comparators were used to determine grain size in conjunction with magnification with standard Bosch and Lomb® 40x hand lenses. All cores were wetted for color determination to show true color. Diluted hydrochloric acid was used to test for the presence of carbonates on freshly etched surfaces. Engineering rulers were used to measure bedding and zone thicknesses.

Figure 9: Core samples as received in boxes with place-holders for missing section.

3.4 DATA COMPILATION

Strater® by Golden Software® was used to compile the MSCL, hand sample, and medical CT data into lithologic logs that fit onto single pages. Some of this data can be accessed from NETL's Energy Data eXchange (EDX) online system (https://edx.netl.doe.gov) using the following link: https://edx.netl.doe.gov/dataset/martinsburg-formation-ct-data. The process included normalizing the data relative to actual core thickness and creating templates that would automatically read in data-streams from multiple sources. This process enabled consistent and systematic data compilation for all 9 samples. The industrial CT data was not included because of its 3D nature and because the complex methodology used to display such data does not lend itself to print.

3.5 INDUSTRIAL CT

High resolution, feature-scale computed tomography was performed with a North-Star Imaging Inc. M-5000® Industrial Computed Tomography System (industrial CT). The system was used to obtain higher resolution scans, ranging from 30–42 µm per pixel, and thus provide a better

understanding of specific features. The two primary limitations, which made sample selection critical, were the limited region of interest that can be scanned at one time (less than 3 in.) and the length of time, in excess of 90 min per sample that it takes to scan. Sections were chosen for industrial scanning based on the presence of notable features such as factures, pore space, unique mineralogy, and apparent lithologic transitions.

The scans were performed at a voltage of 185 kV and a current of 400 µA, which provided the best balance of resolution and energy to penetrate the samples. The samples were rotated 360° and 1440 radiograph projections of the samples were obtained, averaging 3 individual radiographs at each step to create the reconstruction.

3.5.1 Splicing Image Stacks

The industrial CT scanner has superior resolution, but the improved resolution comes at the cost of limited total scannable area. Many samples that are industrially scanned are greater than 2 in. in length, and have to be scanned in sections. The multiple scans are entirely independent and, as such, it is difficult to make coherent visual representations or systematically consistent volumetric assessments of features within the samples. This is due to inherent grayscale shifts in the visual representations particular to each scan, with shifts being determined by the maximum and minimum x-ray attenuation within each individual scan. Those attenuations coordinate with varying grayscale number assignments, and thus each sample has a unique grayscale histogram that is defined by the density variability within that sample section.

Multiple scans of different sections of a sample are completed with identical settings, such as focal distance, source pitch, etc. If all scan parameters are the same, then the individual scans will have identical resolutions. However, scans are prone to a tilt due to asymmetrical rotation about the primary rotational axis (Figure 10). As the X-ray source moves up the sample, the "wobble" in the rotation increases, which further offsets the scan radiographs. When the wobble is integrated into a 3D representation, it results in the displacement of the primary viewing axis and thus a mirror imaging of radiographs instead of the ideal overlay.

In order to better visualize and understand sample features, a methodology was developed that enables scans to be systematically and consistently spliced together into one coherent image stack. Each scan has to be untilted first, and then grayscale histograms have to be matched to make integration of two sections seamless. The untilting of a stack entails utilizing both the reconstruction software to correct the axis (x-reference) and also using ImageJ (Rasband, 2017) with the untilt stack plugin which shifts each image, sequentially, in the stack along the x and y axis based on the users' defined region of interest. Next, to match the grayscales of the two sections, a common slice is chosen; this common slice acts as the joining point for the two stacks and represents the exact same slice in the volume. The image stacks are then converted to 8-bit grayscale to limit the total histogram range to 255 values. The highest and lowest grayscale valued objects in the representative slices are then examined to determine the range of values and approximate grayscale values of individual features. ImageJ is then used to adjust the brightness and contrast settings on one stack to shift the grayscale ranges to match those of the highest and lowest values on the other stack; in effect, the stacks will have the same grayscale values for the features present such as pores and matrix. Once the stacks have been untilted and their grayscales matched, they can be concatenated into one continuous volume. The continuous volumes allow for the isolation and quantification of features of interest larger than could be captured in an individual industrial CT scan.

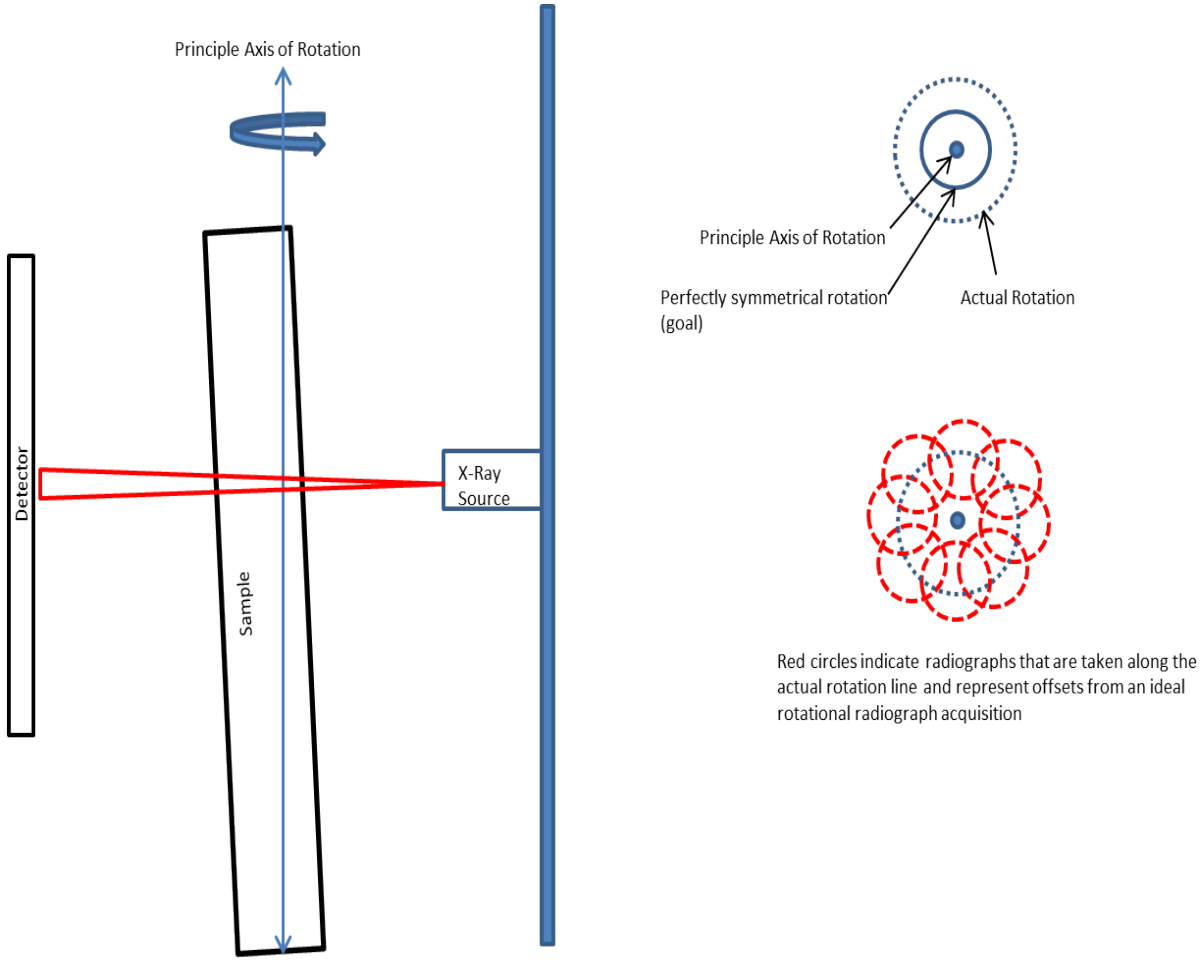

Figure 10: Side view (A) and top view down (B) of rotation inconsistencies with industrial scanner and objects longer than 2 in. that require multiple scans. The illustration shows how the tilt of the sample introduces an offset in the radiographs that increases as you move along the long axis of rotation.

3.5.2 Isolation and Display of Features

The premise of isolating features is to first segment out the feature based on its unique grayscale value. Once this isolation has occurred, the next steps are to differentiate multiple isolated features and then combine them into one coherent visual representation.

First, images are thresholded such that the background, be it mineralogic matrix or open void, is isolated to create an 8-bit binary image. This thresholding creates a “mask” of the features of interest. The mask is then converted to a skeletal outline of the features utilizing the ImageJ Binary Skeletonize function. The resulting skeletonized image is then converted into a 16-bit format; this gives the flexibility to alter the values of the features to values greater than 255.

In order to overlay the images, the original image on which the mask was based is converted to 8-bit and then back to 16-bit; this functions to set all grayscale values to 255 or less, but as

mentioned above allows for the insertion of shapes/lines with values greater than 255. Objects that were isolated are then given values sequentially higher than 255, i.e. 256, 257, etc.

The images are then combined using the ImageJ Image Calculator Transparent-Zero function which transposes the highest value voxels in the resulting image. The caveat of this is that features will overlay each other, with the highest valued feature being the dominant feature; care was taken to ensure that fractures were always the highest value so that they would always crosscut other features in the same fashion as they do within the actual sample. This process is repeated until all features of interest have been added to a final concatenated image.

The look-up table, which is the numerical assignment of colors, is then modified to give each value higher than 255 a distinct, identifiable color. This allows the individual features to be differentiated both from each other and also from the grayscale “background” matrix.

4. RESULTS

Processed 2D slices of the medical CT scans through the cores are shown first, followed by the compiled well logs, and a more detailed description of the industrially CT scanned sections of the Lost River core.

4.1.1 Medical CT Scans

As was discussed previously, the variation in greyscale values observed in the medical CT images indicate changes in the CT number obtained, which is directly proportional to changes in the attenuation and density of the scanned rock (i.e. darker regions are less dense). The greyscale values in the following images were used in an attempt to maximize the variation observed within the core images. Each image has a unique greyscale range, so they should not be interpreted to indicate that a medium grey zone in one image has the same density as a medium grey region in another image. Many qualitative comparisons can be made, however, such as noting bedding planes with different densities or identifying open fractures through the presence of dark zones in the scans.

Core was scanned in 3 ft or smaller sections due to the limitation of how many images could be generated for each scan. In highly-fractured regions sections in excess of 3 ft were often scanned with information saved in both log books and via photographs taken at depths where the breaks in the core were located. In the following images the overall depth for each scanned sub-section of core is listed, but no data is given on the specific locations of the larger breaks in the core to conserve space in this document. In addition, the cores were received in many broken sections with some sections obviously oriented incorrectly; researchers and technicians reassembled fractured sections based on geometry to match the marked depths within the core boxes.

Several items of general interest are listed below.

- The drill shoe was still attached to the Lost River core from Drill Hole #255, as seen at the bottom of the core from depths of 43.5 to 44.9 ft in Figure 25
- A large void space within a fractured zone is noticeable in the Lost River core from Drill Hole #751, in the interval from 35.2 to 36.4 ft as shown in Figure 36

4.1.1.1 Lost River core, Drill Hole #51

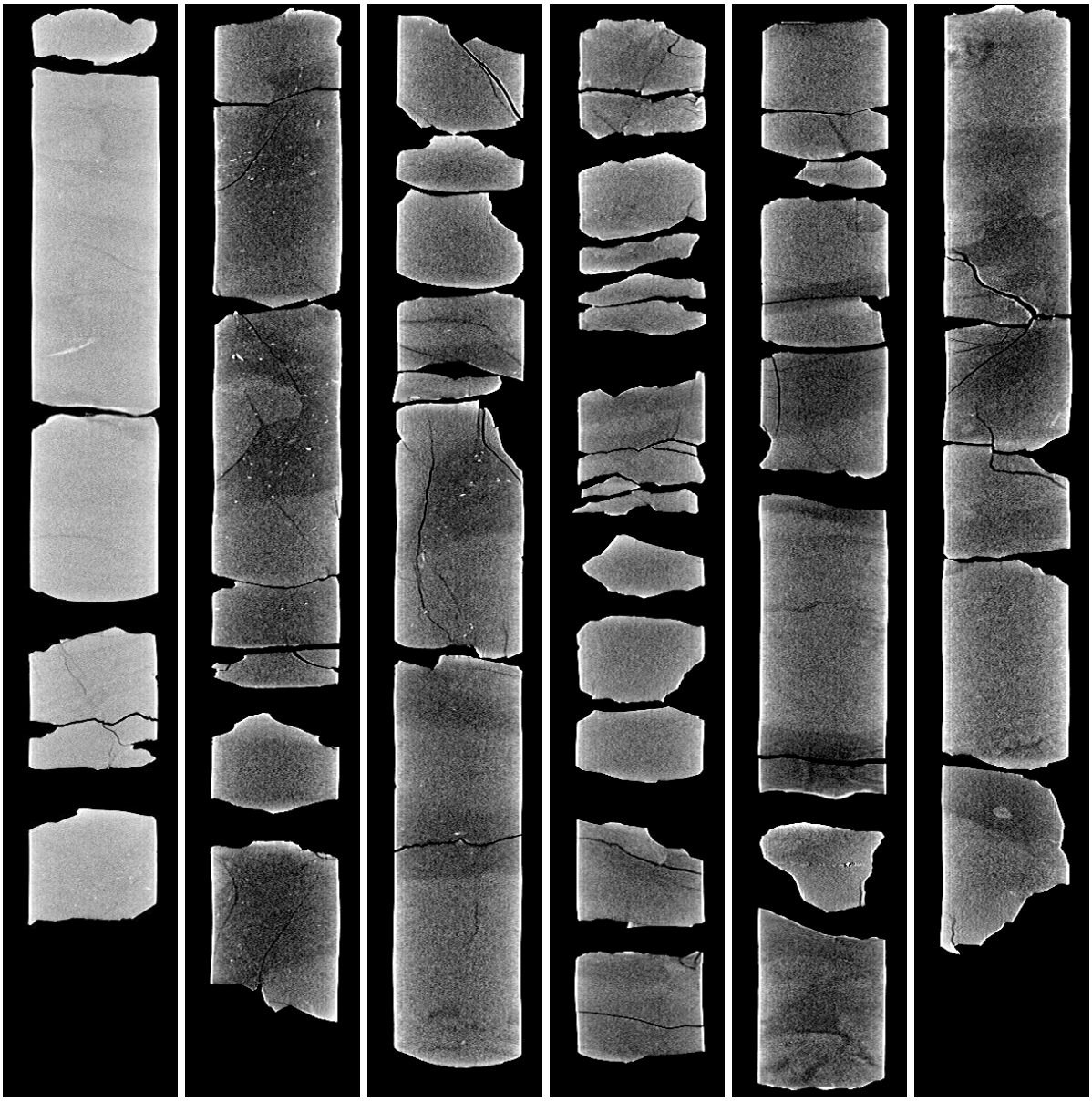

Figure 11: Lost River core Drill Hole #51, medical CT scans from 20.0 to 33.7 ft. Left to right and top to bottom the core depths are 20.0–22.0, 22.1–24.0, 24.1–25.9, 26.0–29.9, 30.0–32.0 and 32.0–33.7 ft.

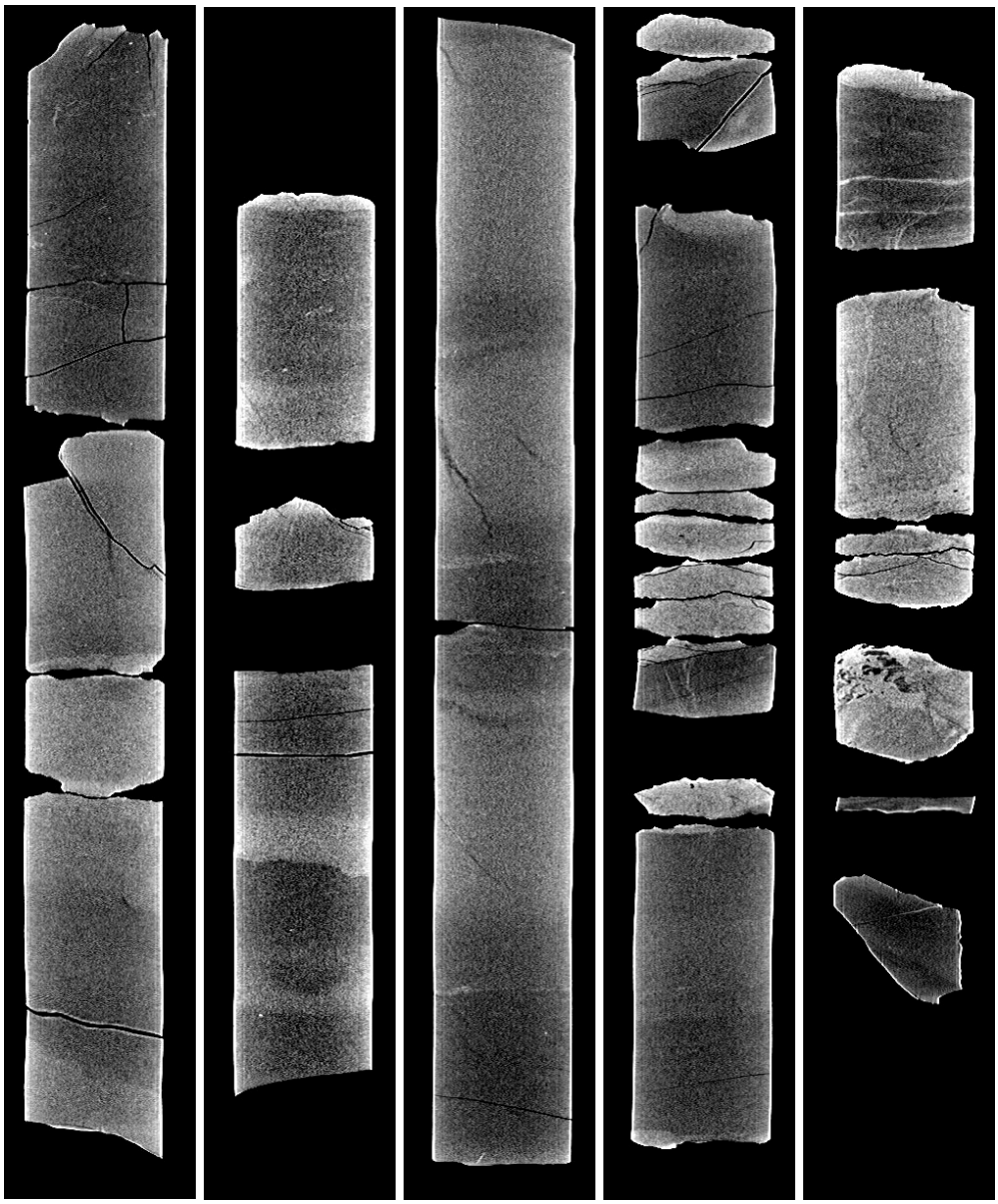

Figure 12: Lost River core Drill Hole #51, medical CT scans from 33.9 to 42.0 ft. Left to right and top to bottom right the core depths are 33.9–35.5, 35.5–37.7, 37.8–39.7, 39.7–41.5, and 41.6–42.0 ft.

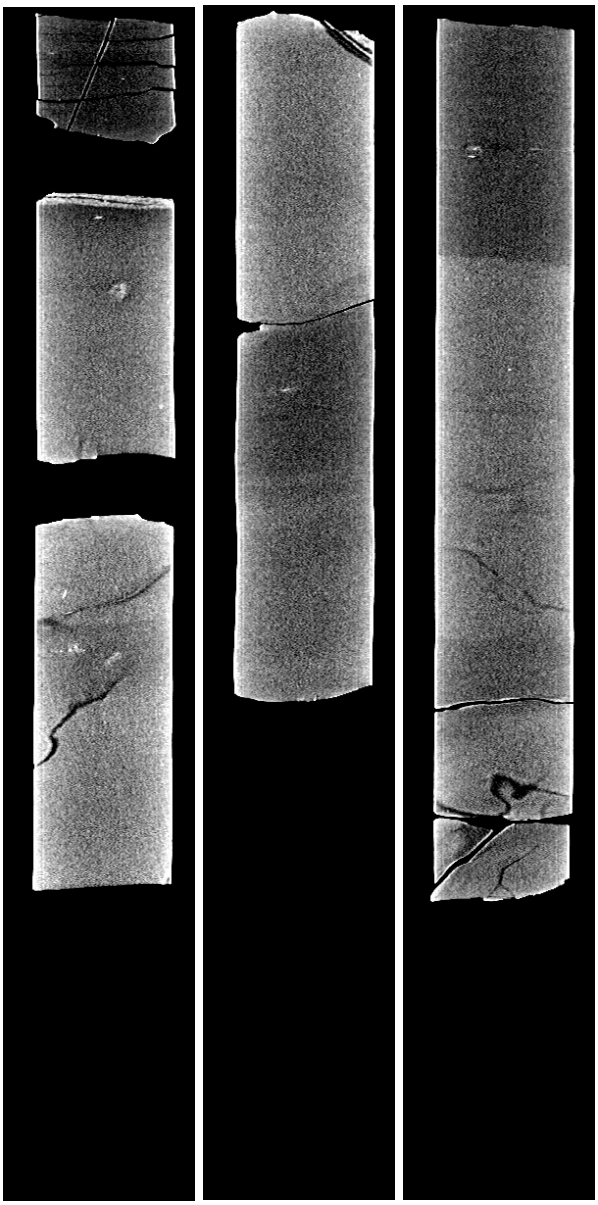

Figure 13: Lost River core Drill Hole #51, medical CT scans from 42.4 to 47.0 ft. Left to right and top to bottom the core depths are 42.4–43.4, 43.7–44.2, and 45.5–47.0 ft.

4.1.1.2 Lost River core, Drill Hole #61

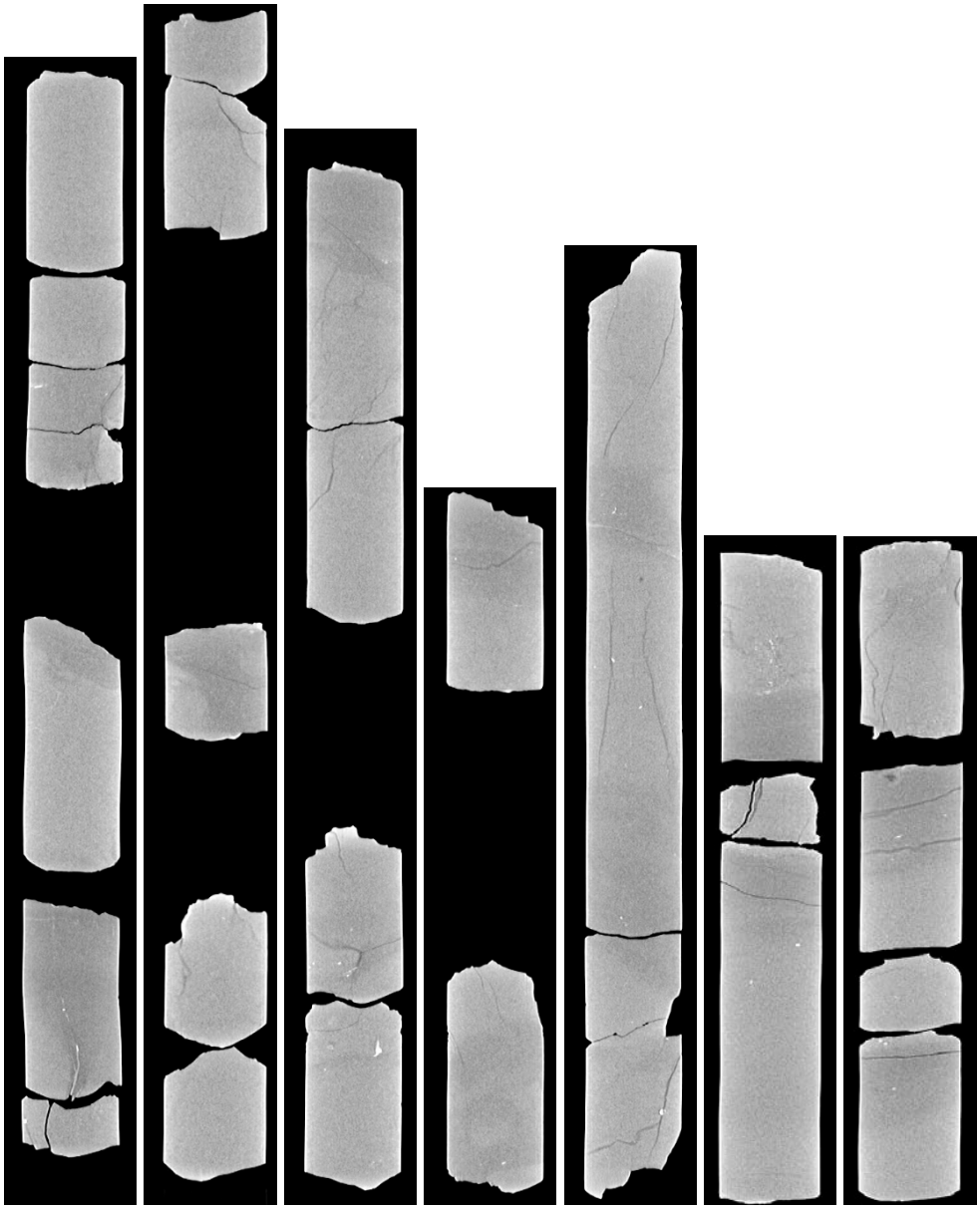

Figure 14: Lost River core Drill Hole #61, medical CT scans from 25.2 to 35.8 ft. Left to right and top to bottom the core depths are 25.2–27.0, 27.0–29.0, 29.0–30.2, 30.2–31.2, 31.2–32.7, 32.7–34.0, and 34.0–35.8 ft.

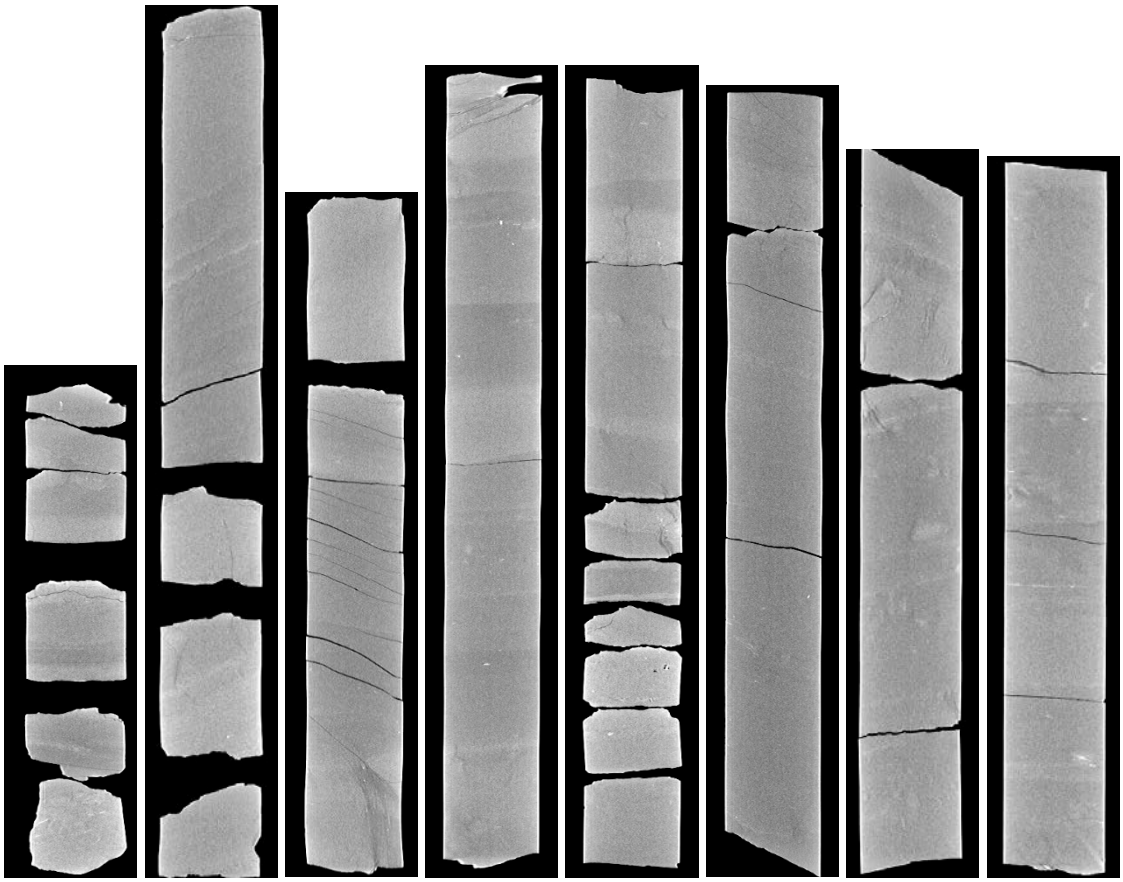

Figure 15: Lost River core Drill Hole #61, medical CT scans from 35.8 to 50.0 ft. Left to right and top to bottom the core depths are 35.8–37.5, 37.5–39.8, 39.8–41.1, 41.1–43.1, 43.1–45.0, 45.0–47.0, 47.0–48.8, and 48.8–50.0 ft.

4.1.1.3 Lost River core, Drill Hole #251

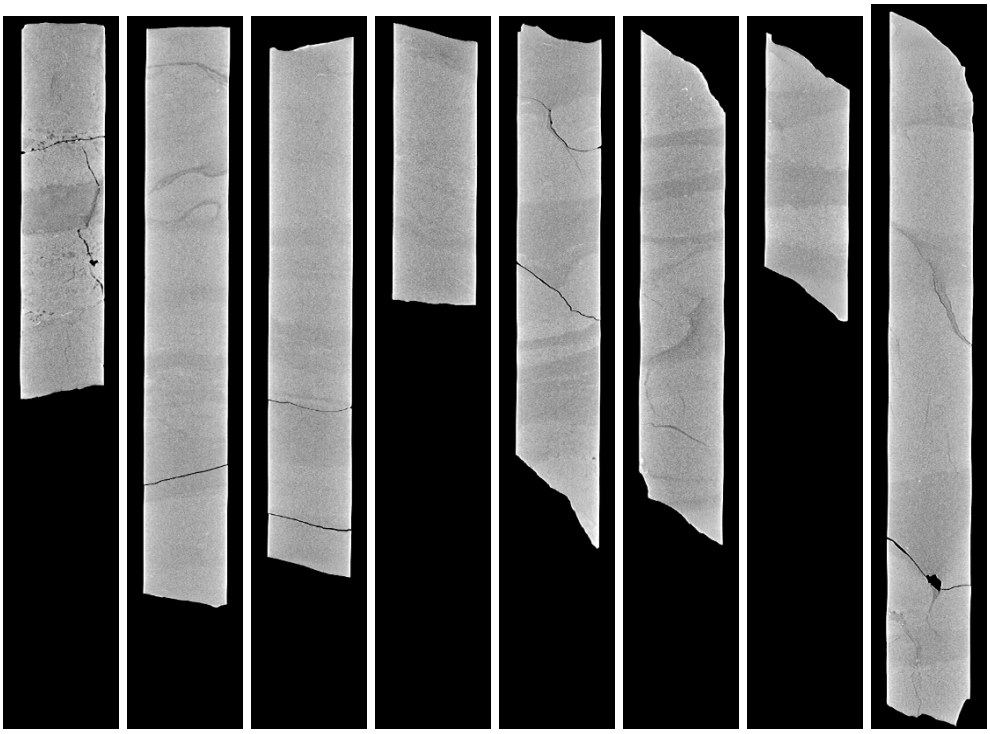

Figure 16: Lost River core Drill Hole #251, medical CT scans from 40.0 to 50.0 ft. Left to right and top to bottom the core depths are 40.0–41.1, 41.1–42.7, 42.7–44.1, 44.1–44.8, 44.8–46.0, 46.0–47.4, 47.4–48.1, and 48.1–50.0 ft.

4.1.1.4 Lost River core, Drill Hole #252

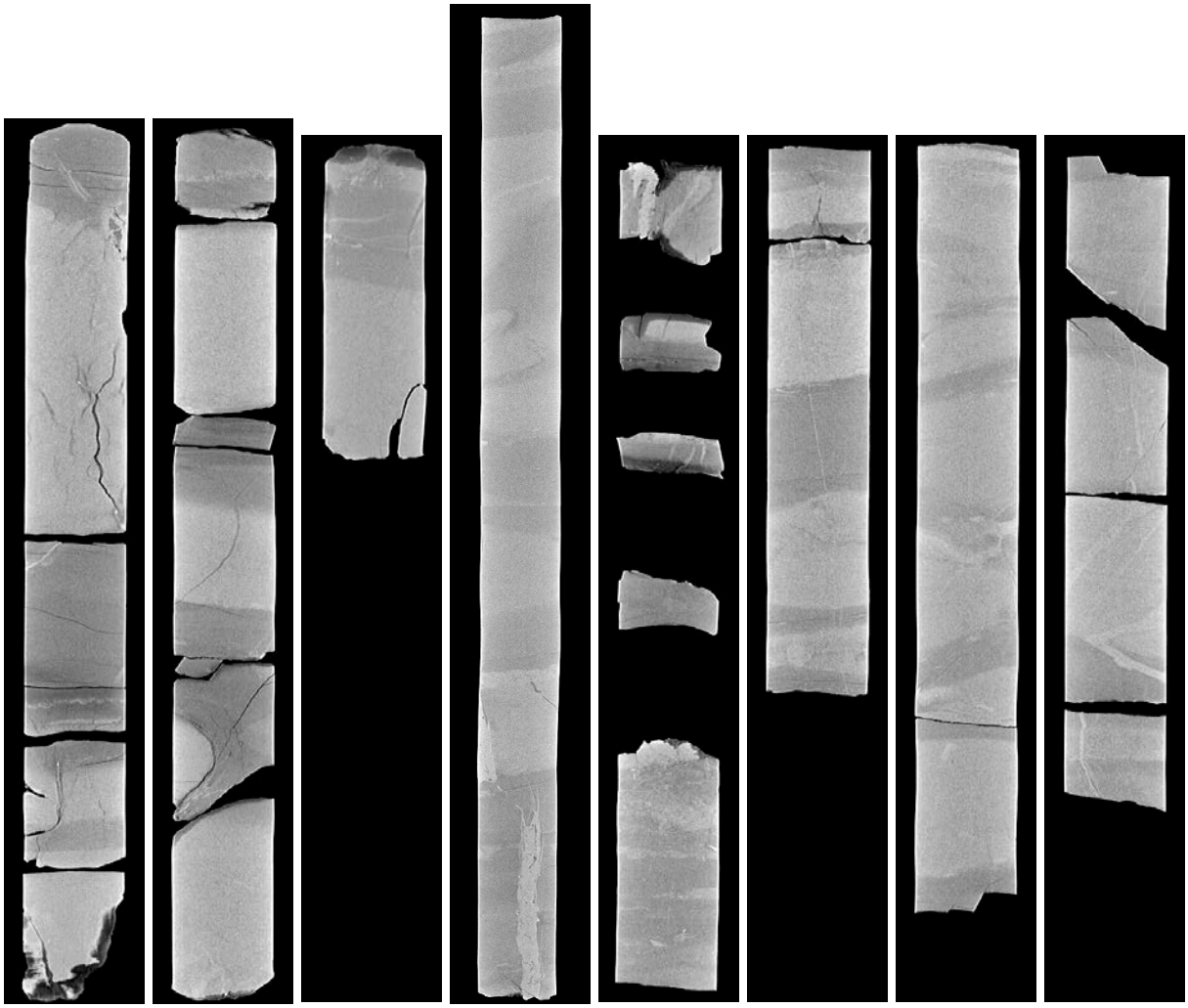

Figure 17: Lost River core Drill Hole #252, medical CT scans from 31.0 to 51.0 ft. Left to right and top to bottom the core depths are 31.0–33.0, 33.0–35.0, 35.0–35.8, 36.0–39.0, 39.0–46.3, 46.3–47.7, 47.7–49.5, and 49.5–51.0 ft.

4.1.1.5 Lost River core, Drill Hole #254

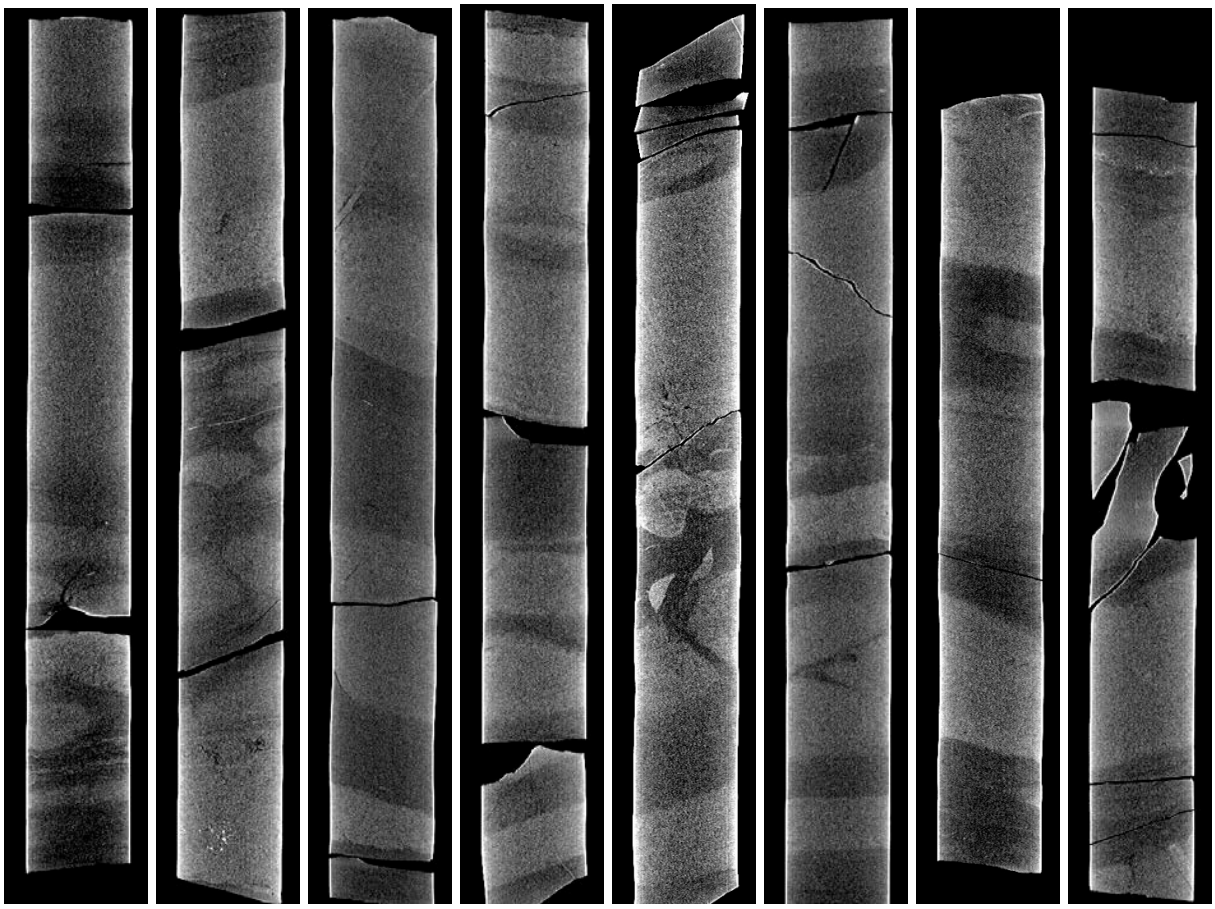

Figure 18: Lost River core Drill Hole #254, medical CT scans from 28.0 to 43.0 ft. Left to right and top to bottom the core depths are 28.0–29.9, 29.9–31.9, 31.9–33.9, 33.9–35.8, 35.8–38.0, 38.0–40.1, 40.3–41.8, 41.8–43.0 ft.

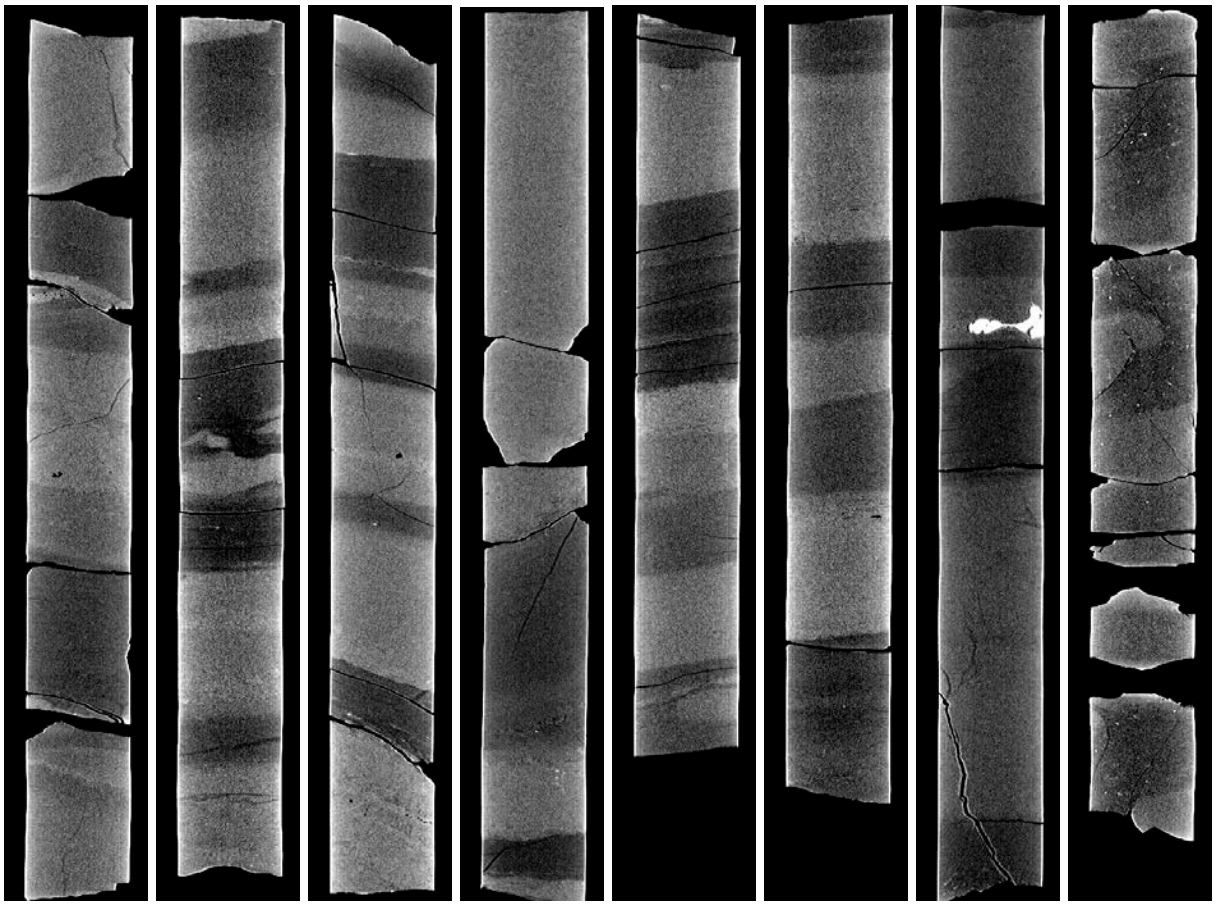

Figure 19: Lost River core Drill Hole #254, medical CT scans from 43.0 to 58.2 ft. Left to right and top to bottom the core depths are 43.0–45.1, 45.1–47.2, 47.2–49.2, 49.2–51.2, 51.2–52.9, 52.9–54.6, 54.6–56.3, and 56.3–58.2 ft.

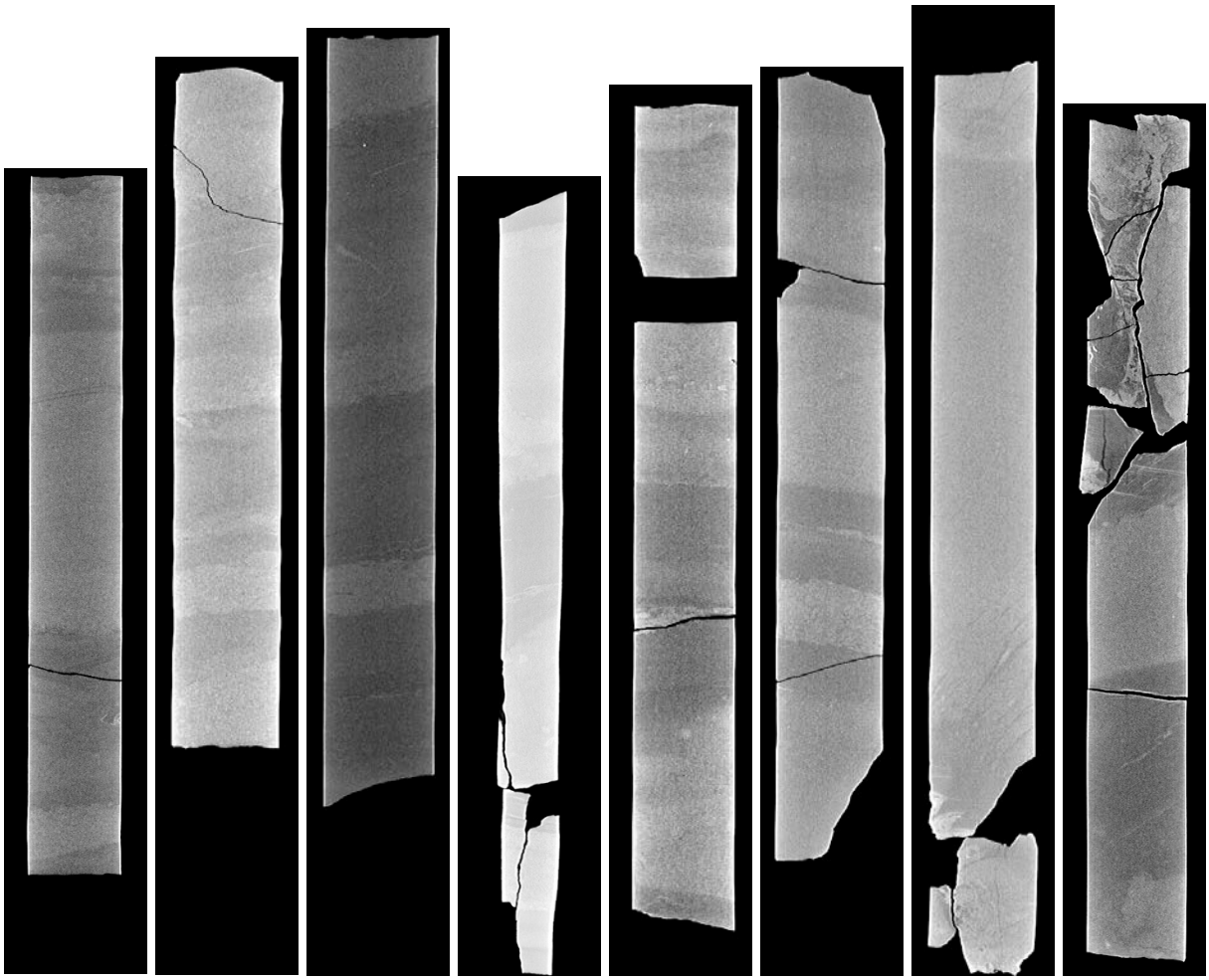

Figure 20: Lost River core Drill Hole #254, medical CT scans from 58.2 to 72.0 ft. Left to right and top to bottom the core depths are 58.2–60.0, 60.0–61.5, 61.5–63.2, 63.2–64.6, 64.6–66.3, 66.3–68.1, 68.1–70.0, and 70.0–72.0 ft.

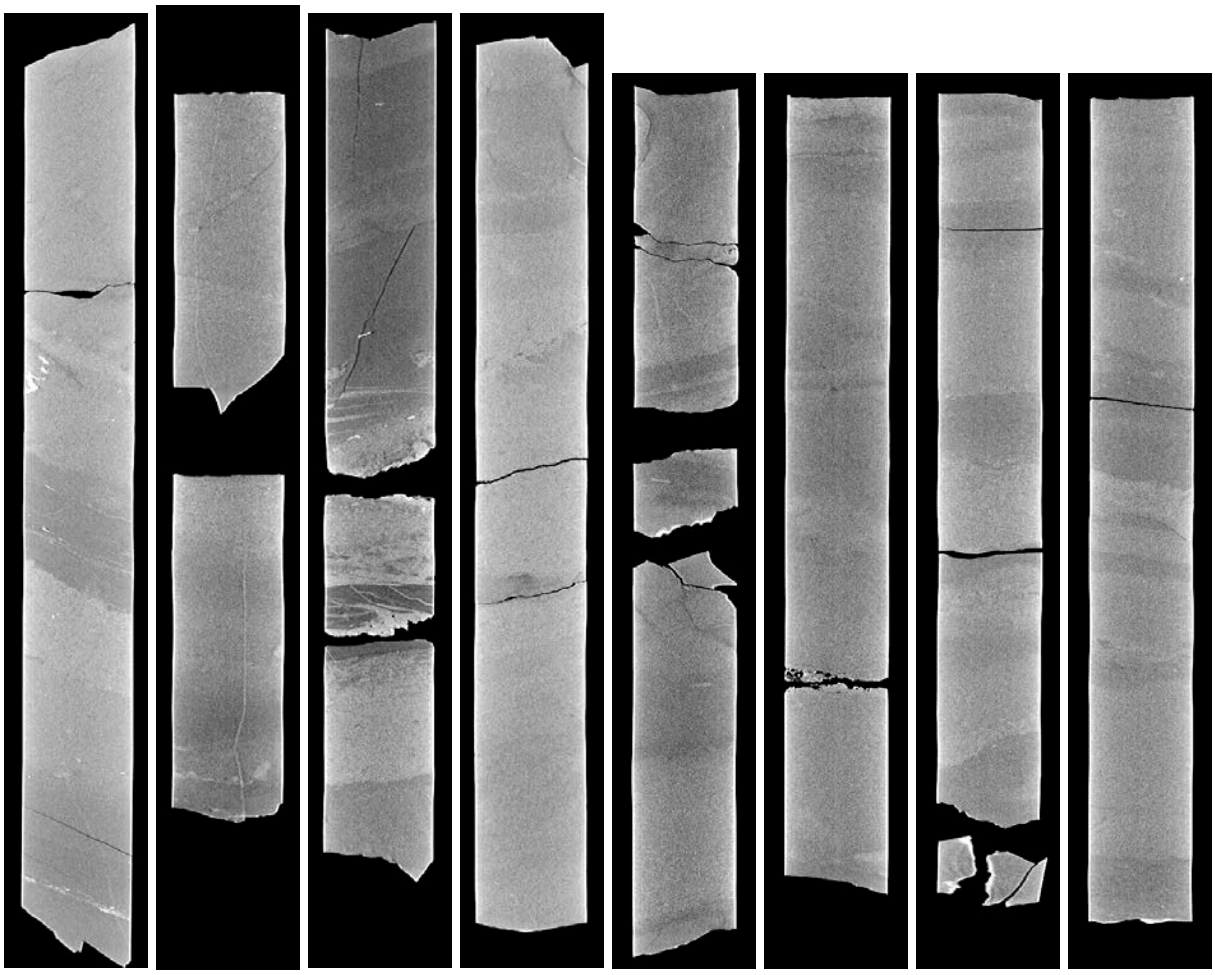

Figure 21: Lost River core Drill Hole #254, medical CT scans from 72.0 to 87.0 ft. Left to right and top to bottom the core depths are 72.0–74.0, 74.0–75.7, 75.7–77.6, 77.6–79.5, 79.5–81.0, 81.0–82.8, 82.8–85.0, and 85.0–87.0 ft.

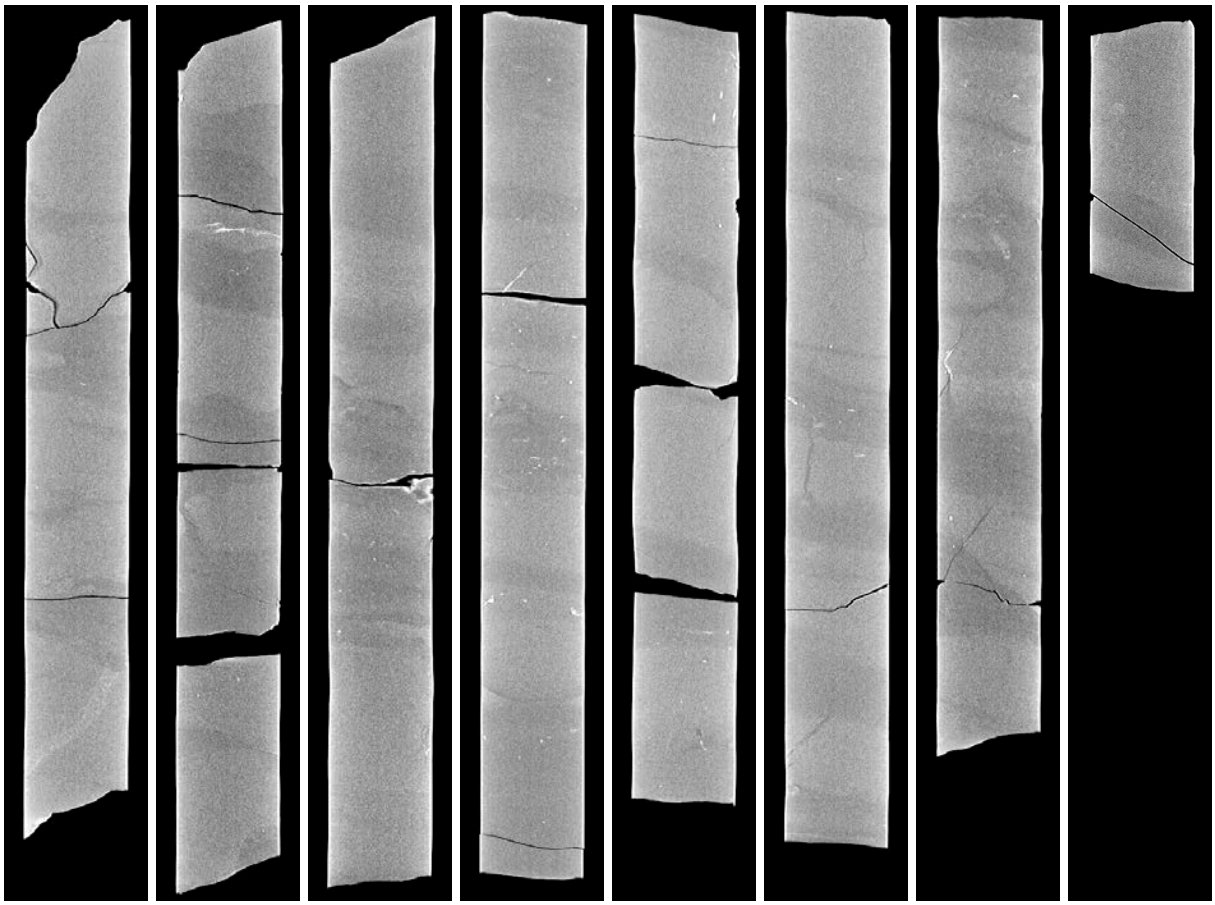

Figure 22: Lost River core Drill Hole #254, medical CT scans from 87.0 to 100.0 ft. Left to right and top to bottom the core depths are 87.0–88.7, 88.7–90.5, 90.5–92.4, 92.4–94.4, 94.4–96.2, 96.2–97.9, 97.9–99.4, and 99.4–100.0 ft.

4.1.1.6 Lost River core, Drill Hole #255

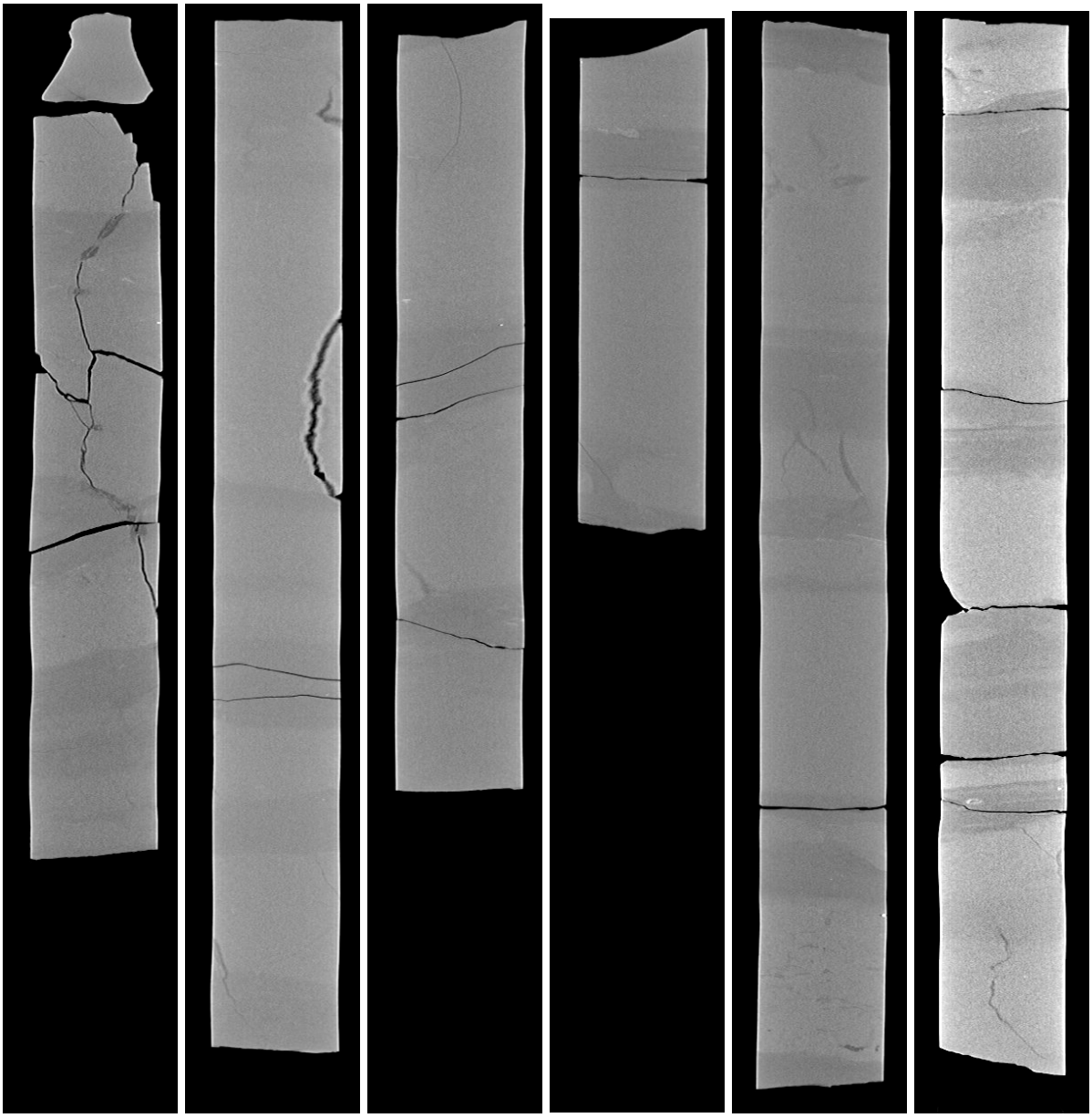

Figure 23: Lost River core Drill Hole #255, medical CT scans from 16.0 to 25.6 ft. Left to right and top to bottom the core depths are 16.0–17.5, 17.5–19.6, 19.6–20.9, 20.9–21.7, 21.7–23.6, and 23.6–25.6 ft.

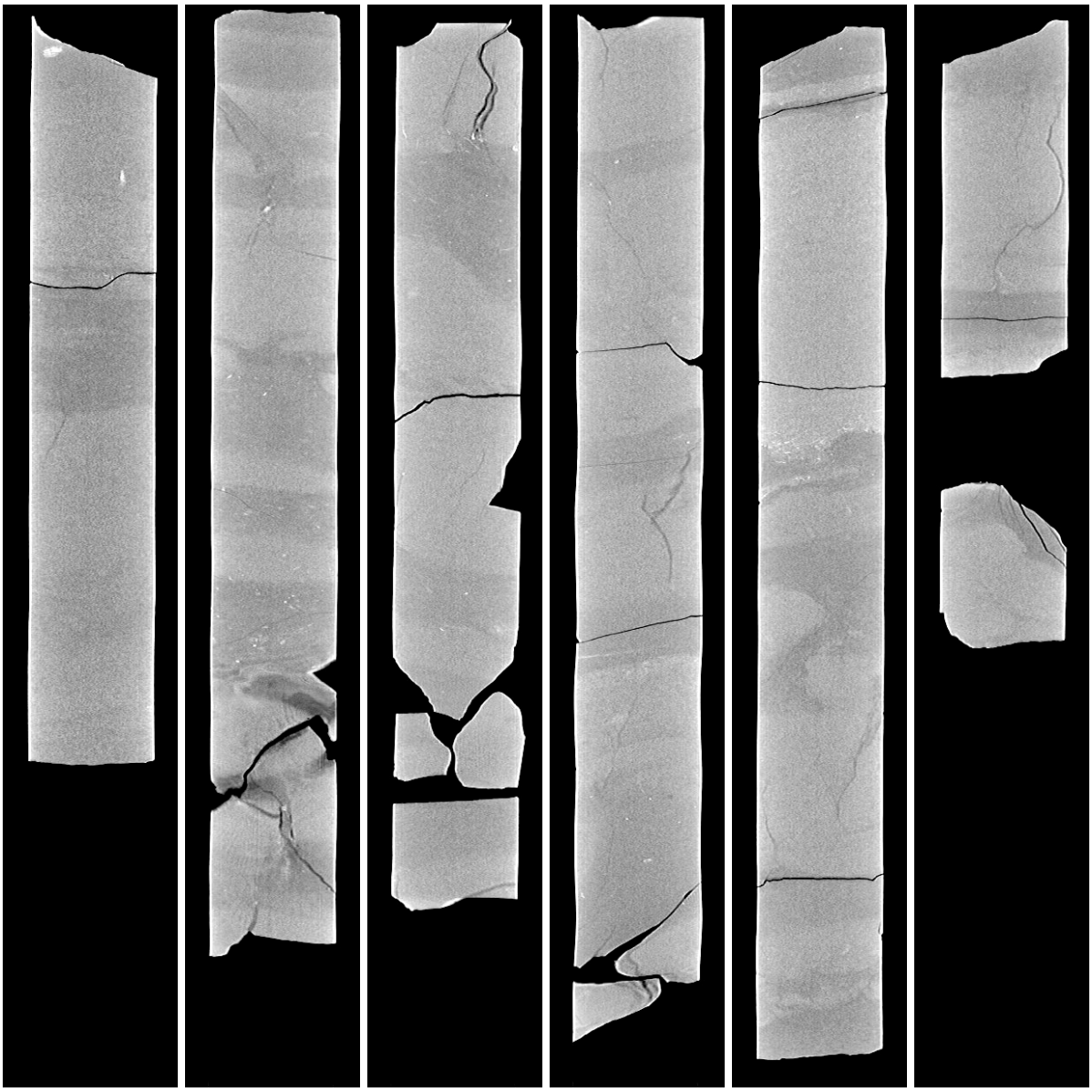

Figure 24: Lost River core Drill Hole #255, medical CT scans from 25.6 to 35.4 ft. Left to right and top to bottom the core depths are 25.6–26.9, 26.9–28.6, 28.6–30.2, 30.2–32.3, 32.3–34.2, and 34.2–35.4 ft.

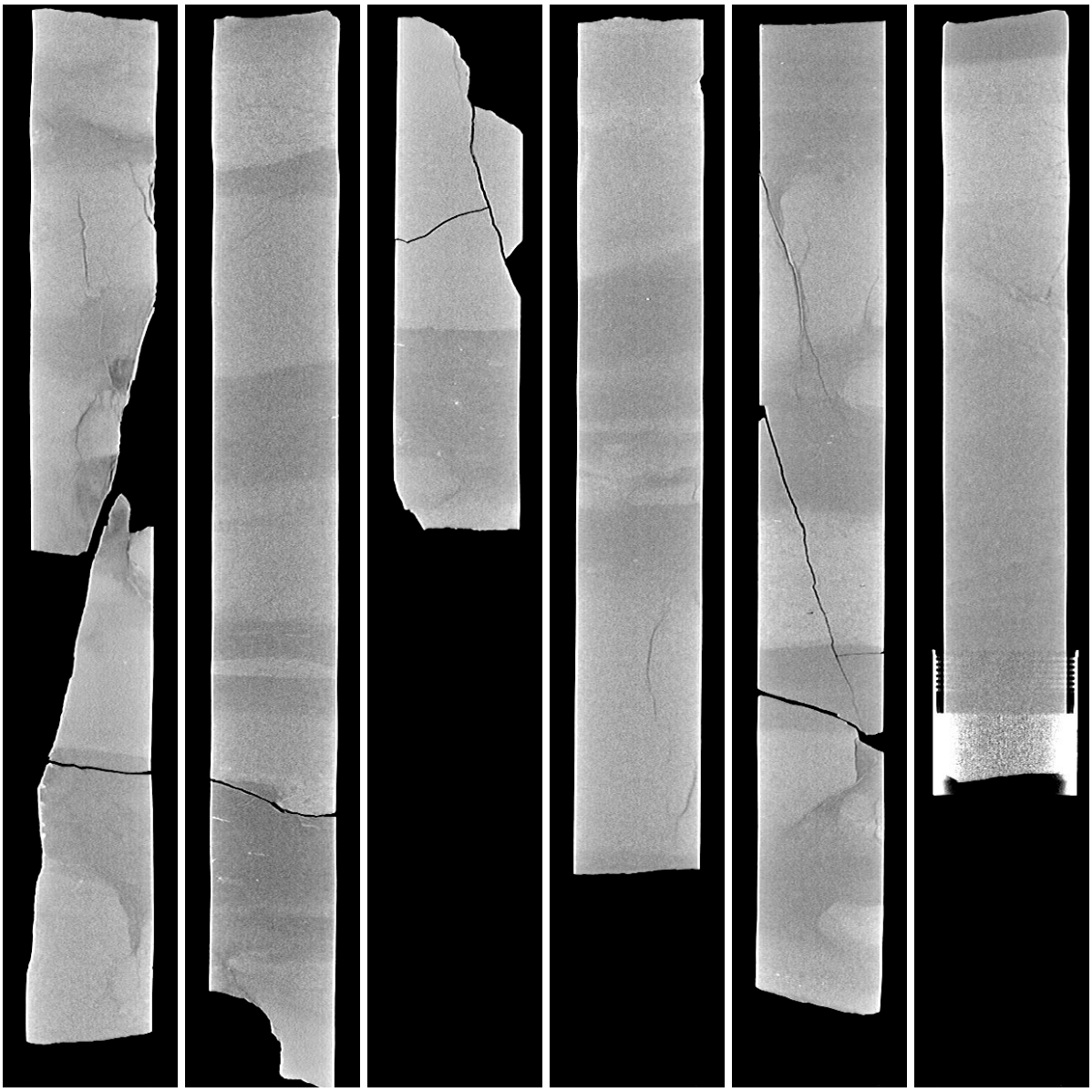

Figure 25: Lost River core Drill Hole #255, medical CT scans from 35.4 to 44.9 ft. Left to right and top to bottom the core depths are 35.4–36.7, 36.7–38.5, 38.5–39.5, 40.0–41.6, 41.6–43.5, and 43.5–44.9 ft.

4.1.1.7 Lost River core, Drill Hole #256

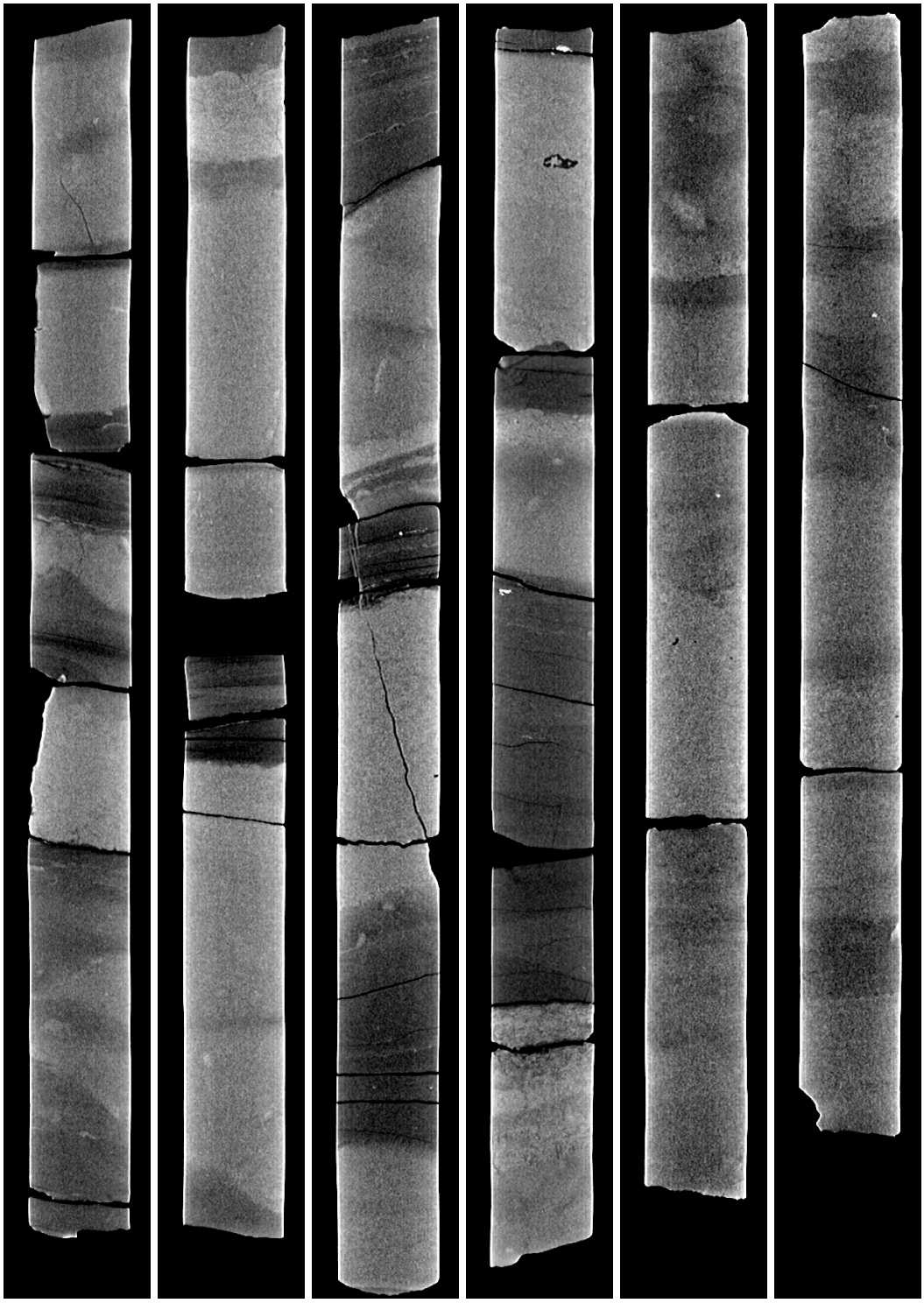

Figure 26: Lost River core Drill Hole #256, medical CT scans from 18.0 to 29.1 ft. Left to right and top to bottom the core depths are 18.0–19.6, 19.6–21.3, 21.3–23.2, 23.2–25.5, 25.5–27.4, and 27.4–29.1 ft.

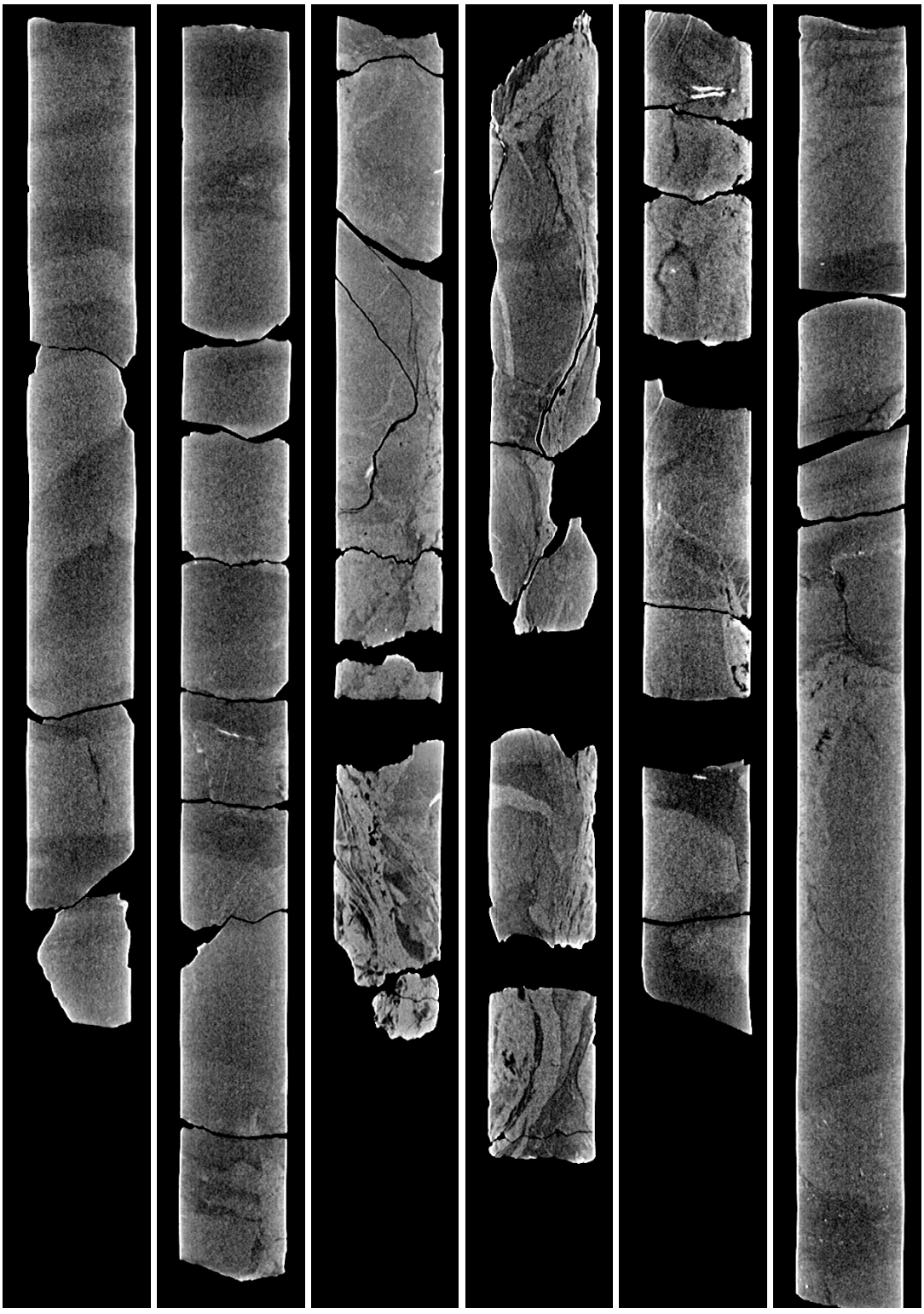

Figure 27: Lost River core Drill Hole #256, medical CT scans from 29.1 to 39.9 ft. Left to right and top to bottom the core depths are 29.1–30.5, 30.5–32.4, 32.4–34.6, 34.6–36.5, 36.5–37.8, and 37.9–39.9 ft.

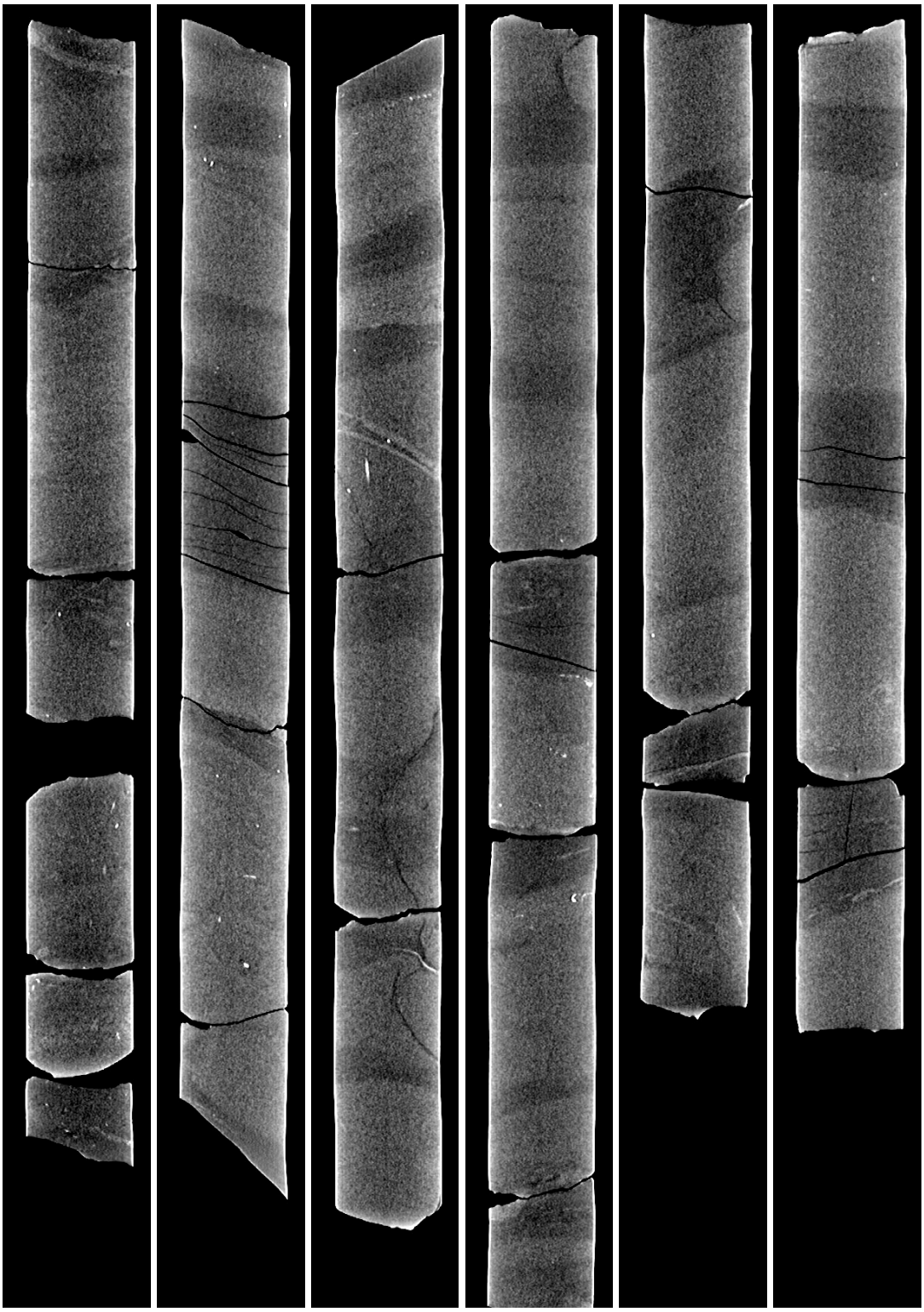

Figure 28: Lost River core Drill Hole #256, medical CT scans from 39.9 to 49.2 ft. Left to right and top to bottom the core depths are 39.9–41.0, 41.0–42.6, 42.6–44.6, 44.6–46.5, 46.6–47.2, and 47.6–49.2 ft

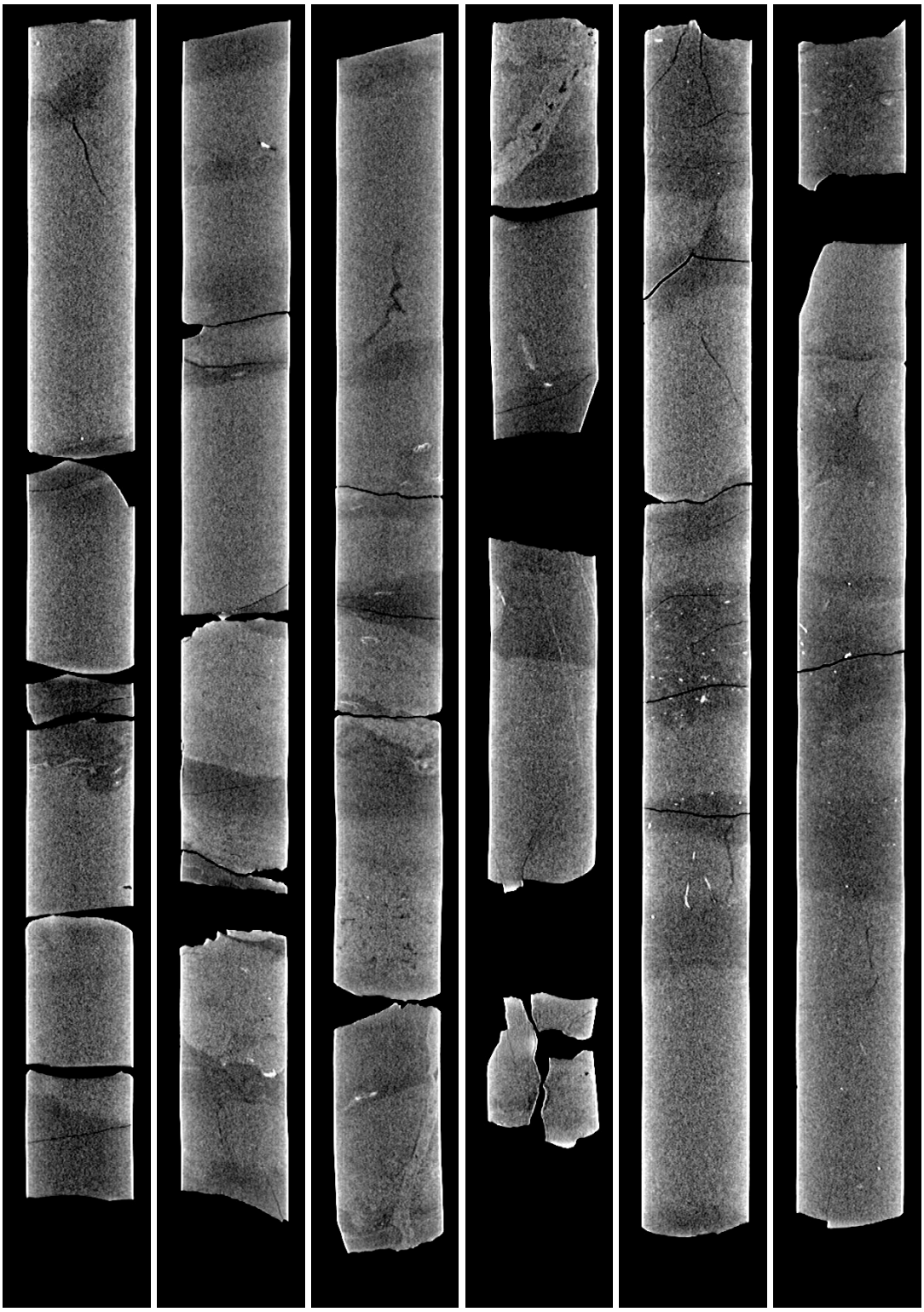

Figure 29: Lost River core Drill Hole #256, medical CT scans from 49.2 to 60.0 ft. Left to right and top to bottom the core depths are 49.2–51.4, 51.7–53.4, 53.4–55.4, 55.4–56.2, 56.2–58.2, and 58.2–60.0 ft.

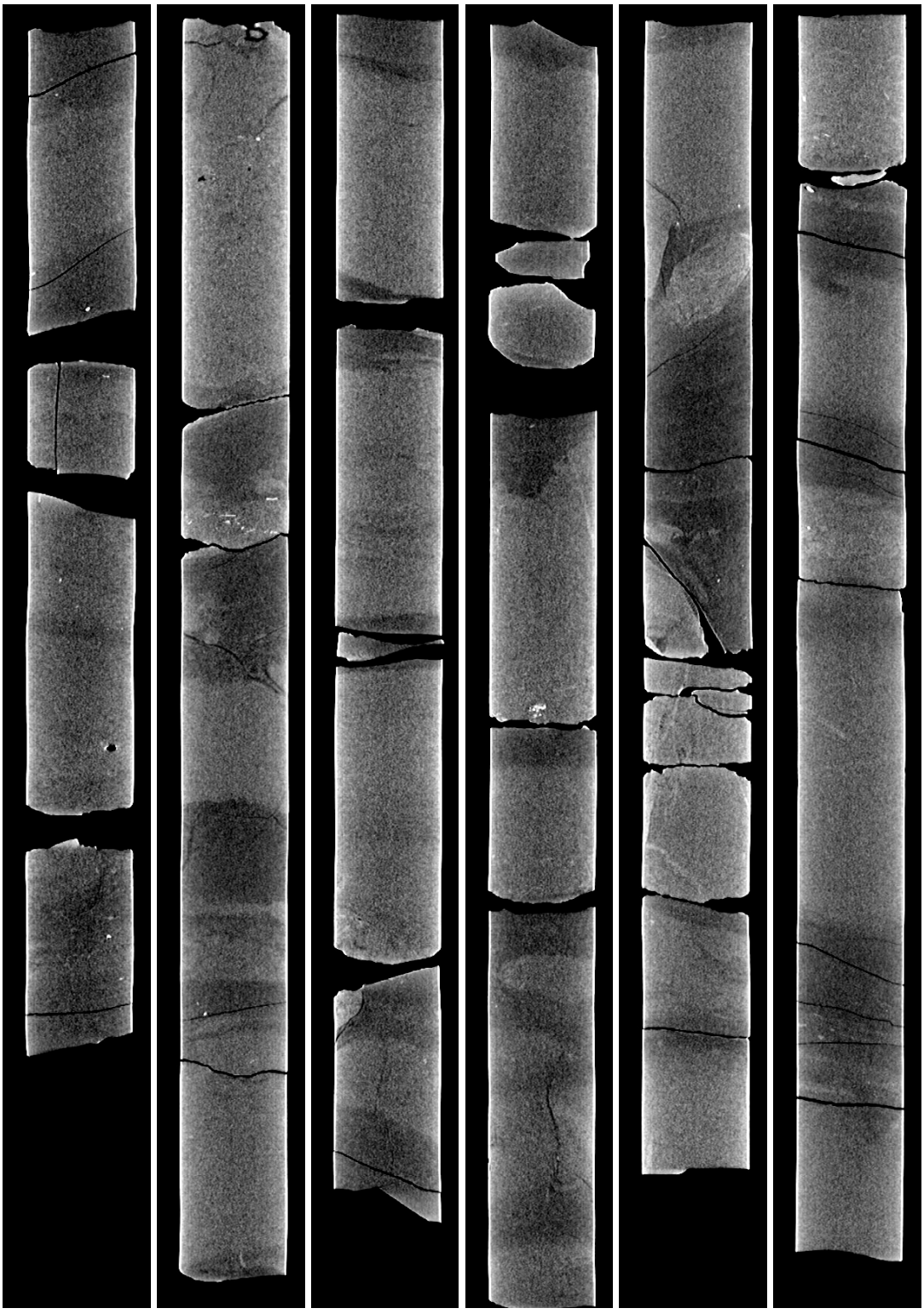

Figure 30: Lost River core Drill Hole #256, medical CT scans from 60.0 to 70.5 ft. Left to right and top to bottom the core depths are 60.0–61.5, 61.5–63.5, 63.5–65.0, 65.0–66.8, 66.8–68.6, and 68.6–70.5 ft.

4.1.1.8 Lost River core, Drill Hole #651

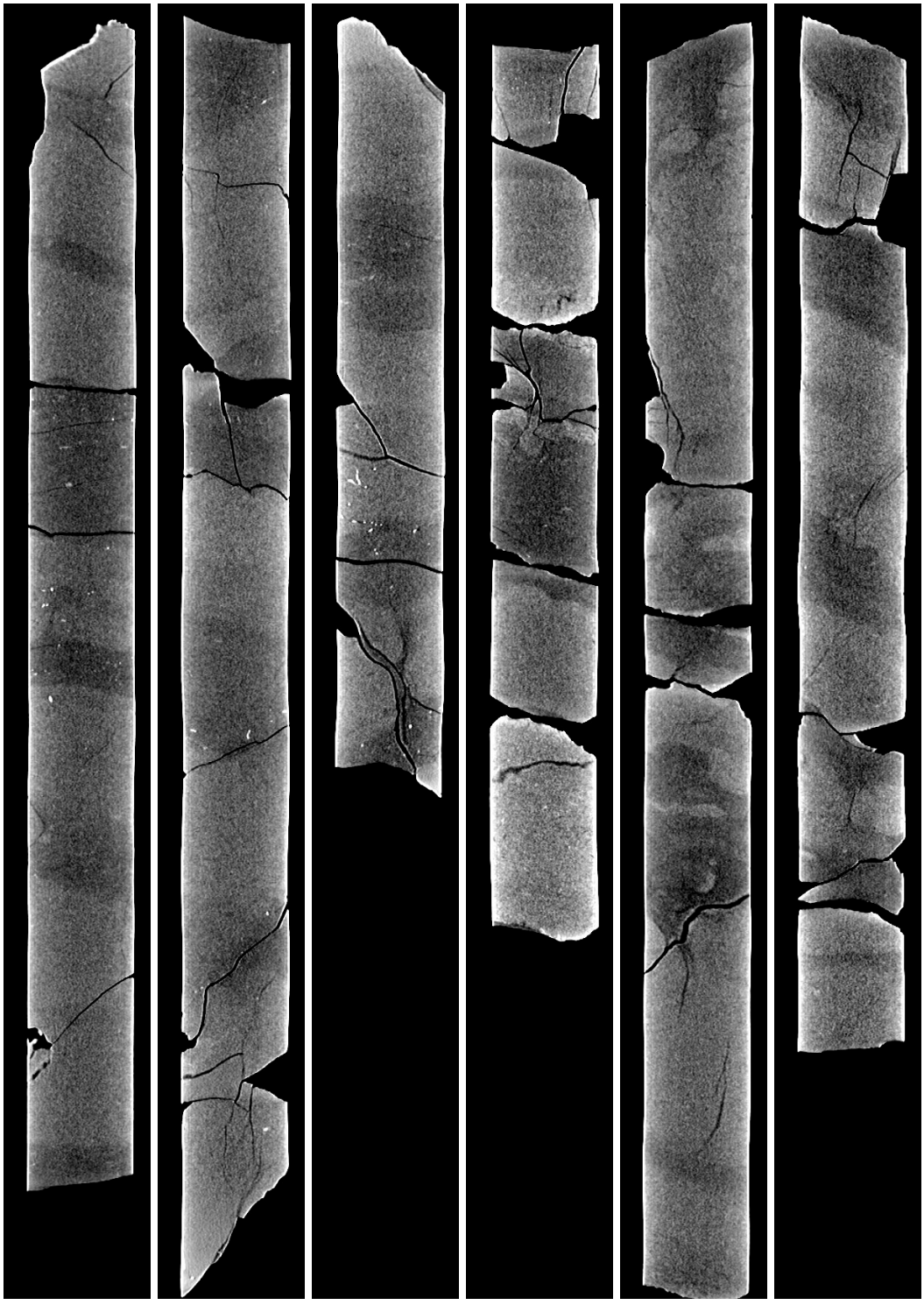

Figure 31: Lost River core Drill Hole #651, medical CT scans from 10.0–19.6 ft. Left to right and top to bottom the core depths are 10.0–11.8, 11.8–13.2, 13.2–14.8, 14.8–16.0, 16.0–18.1, and 18.1–19.6 ft.

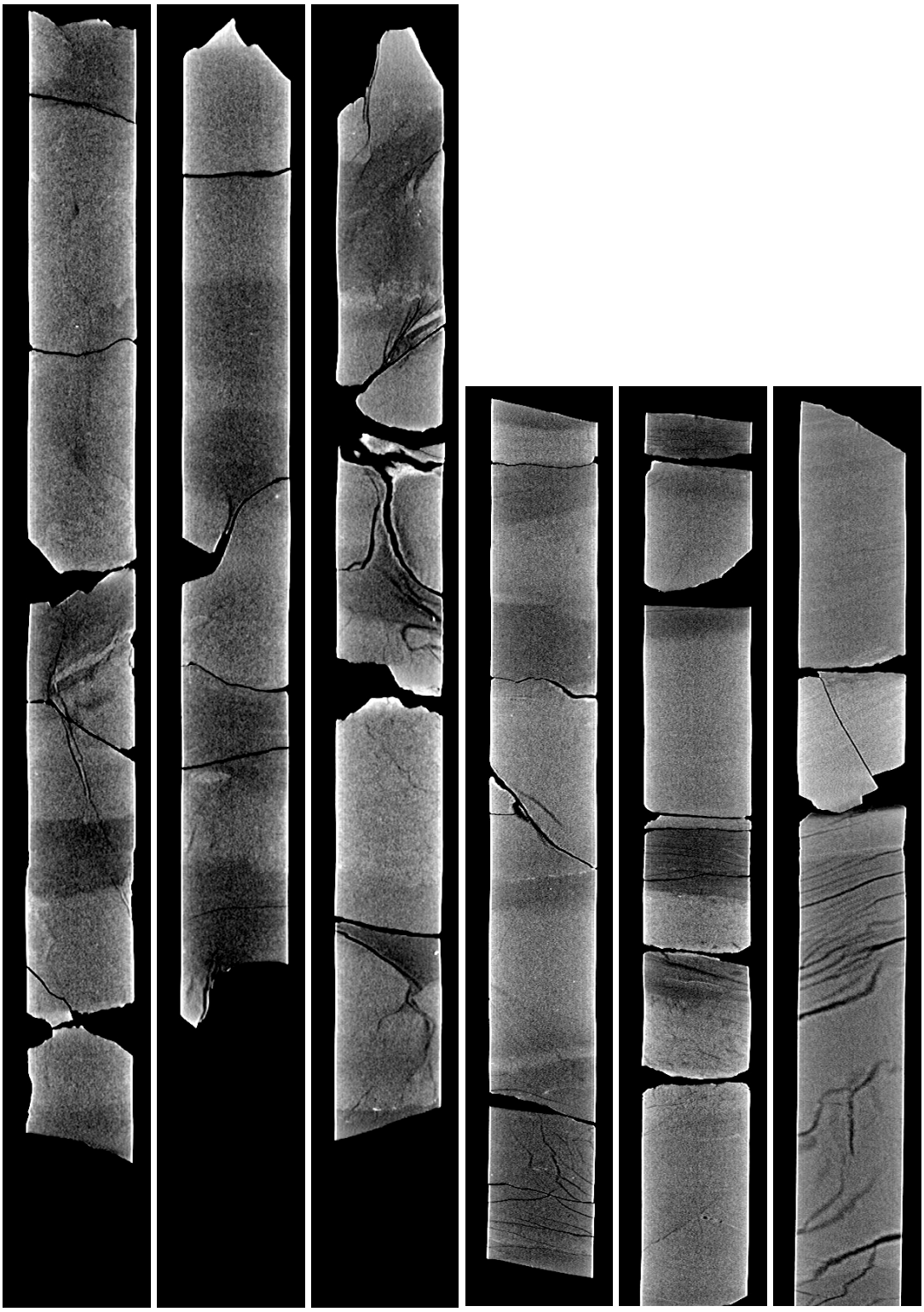

Figure 32: Lost River core Drill Hole #651, medical CT scans from 19.6–31.7 ft. Left to right and top to bottom the core depths are 19.6–21.5, 21.5–23.3, 23.3–25.0, 25.0–27.3, 27.3–29.5, and 29.6–31.7 ft.

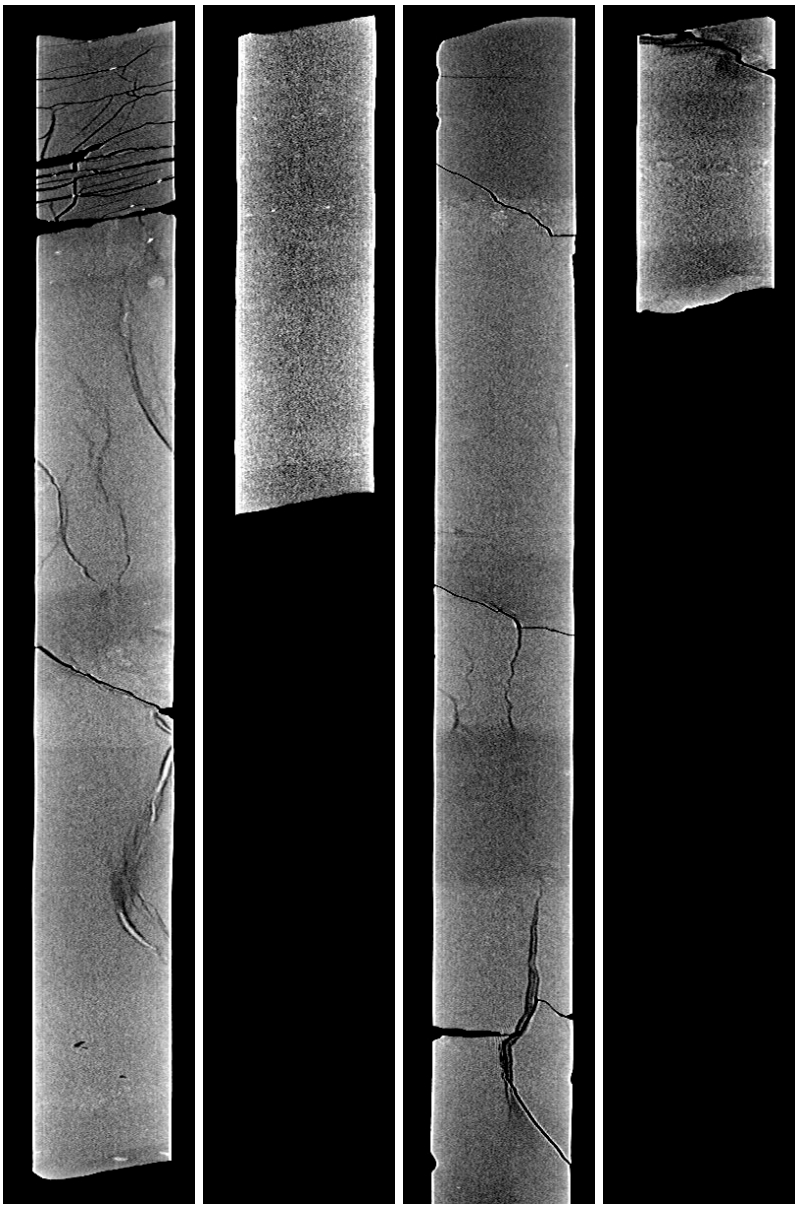

Figure 33: Lost River core Drill Hole #651, medical CT scans from 31.7–40.0 ft. Left to right and top to bottom the core depths are 31.7–33.6, 33.6–35.5, 35.5–36.2, and 36.2–40.0 ft.

4.1.1.9 Lost River core, Drill Hole #751

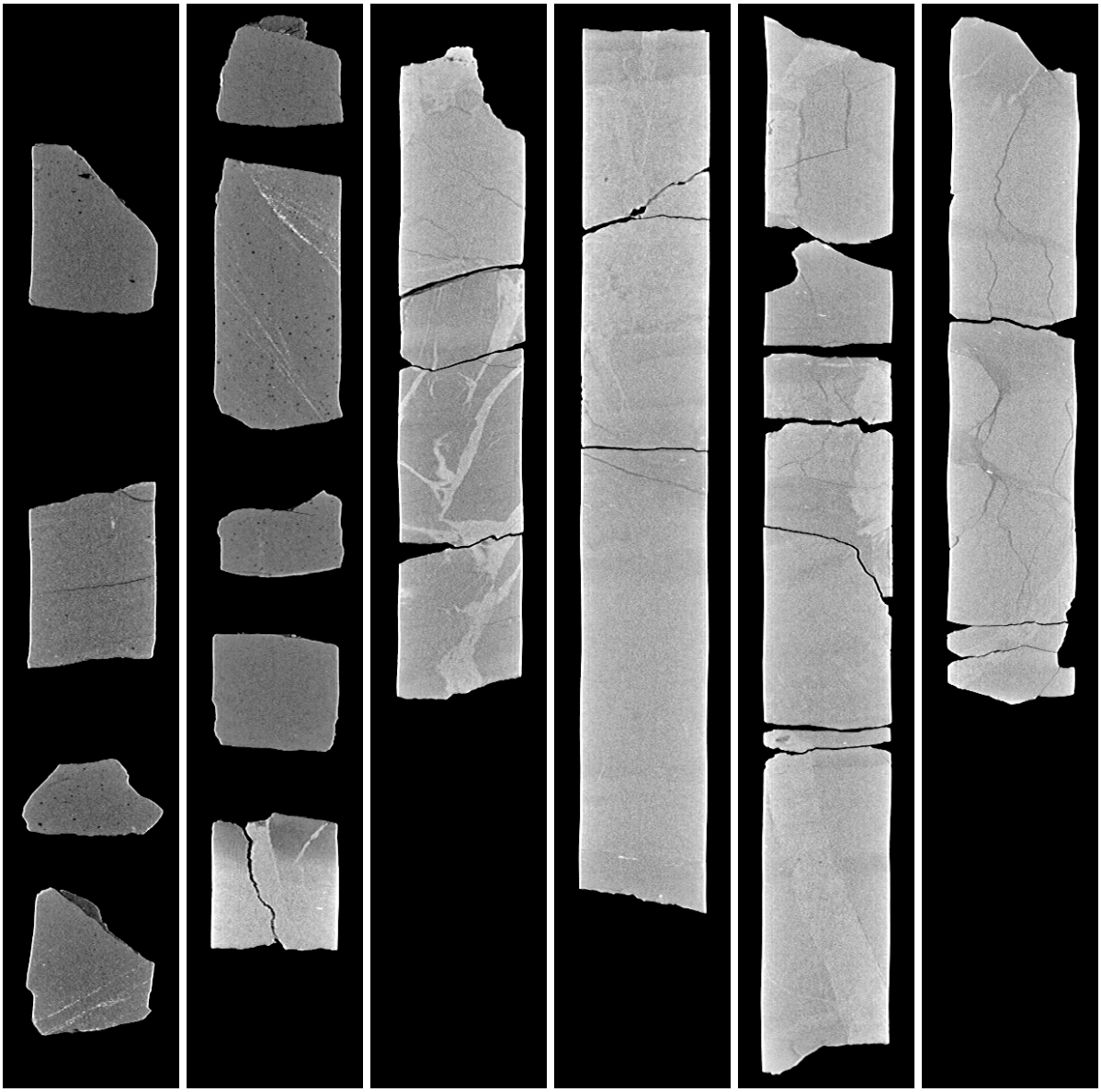

Figure 34: Lost River core Drill Hole #751, medical CT scans from 11.5–23.8 ft. Left to right and top to bottom the core depths are 11.5–16.0, 16.0–17.7, 17.7–19.0, 19.0–20.7, 20.7–22.6, and 22.6–23.8 ft.

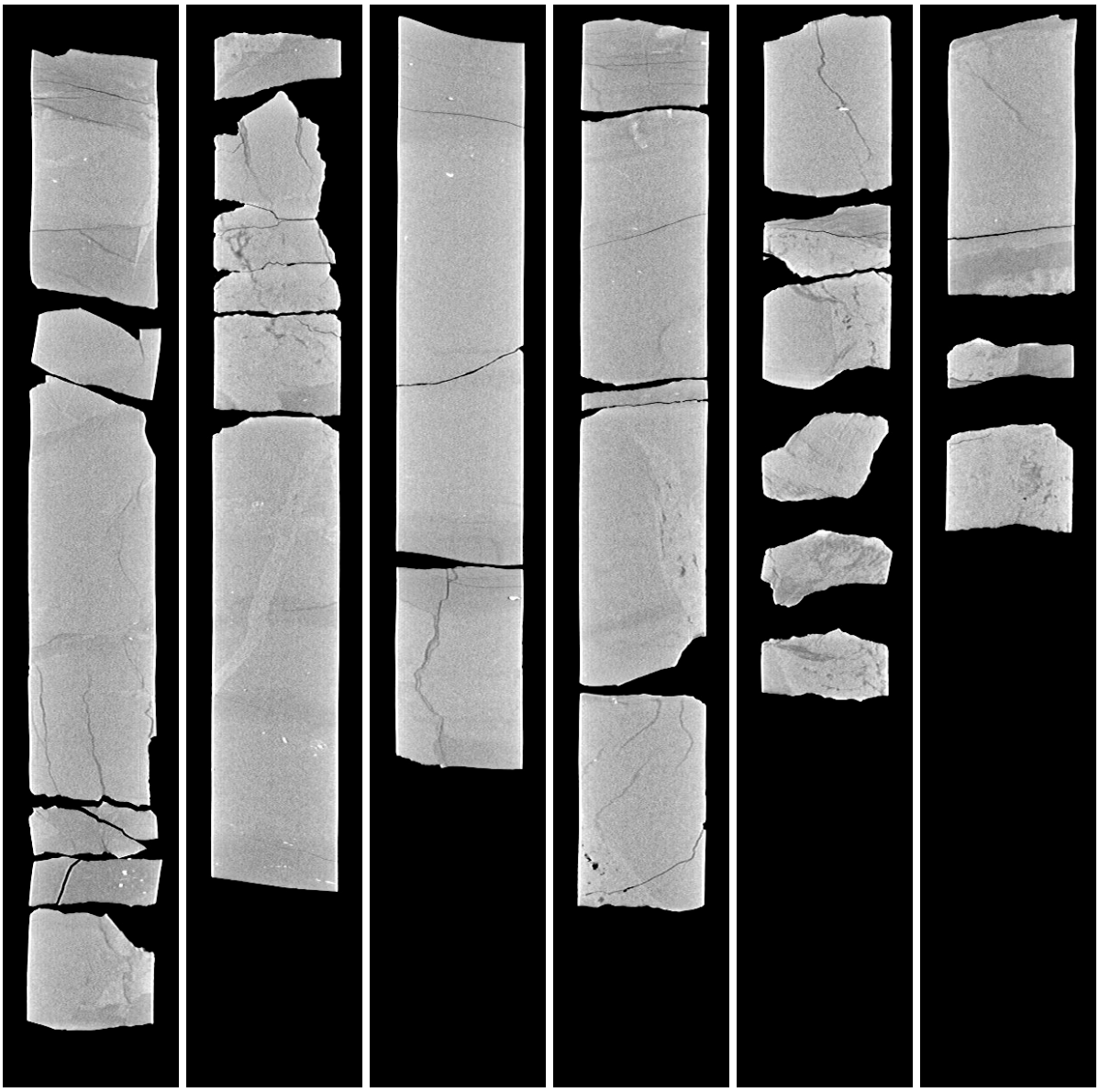

Figure 35: Lost River core Drill Hole #751, medical CT scans from 24.4–33.0 ft. Left to right and top to bottom the core depths are 24.4–26.0, 26.0–27.0, 27.0–28.5, 28.5–30.0, 30.0–32.0, and 32.0–33.0 ft.

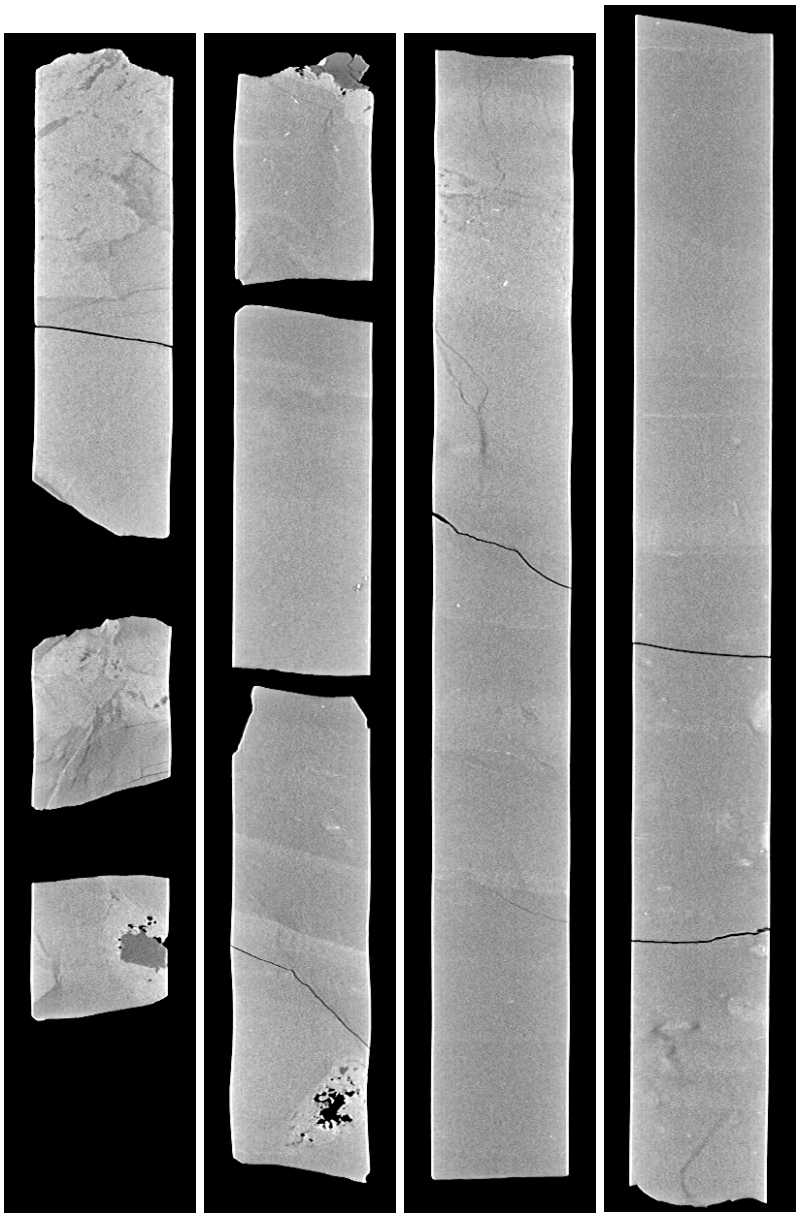

Figure 36: Lost River core Drill Hole #751, medical CT scans from 33.0 to 42.0 ft. Left to right and top to bottom the core depths are 33.0–35.2, 35.2–36.4, 38.0–40.0, and 40.0–42.0 ft.

4.1.2 Compiled Core Logs

The compiled core logs were designed to fit on single pages for rapid analysis of the combined data from the medical CT scans, MSCL readings, and geologic evaluations. These are presented in the following images.

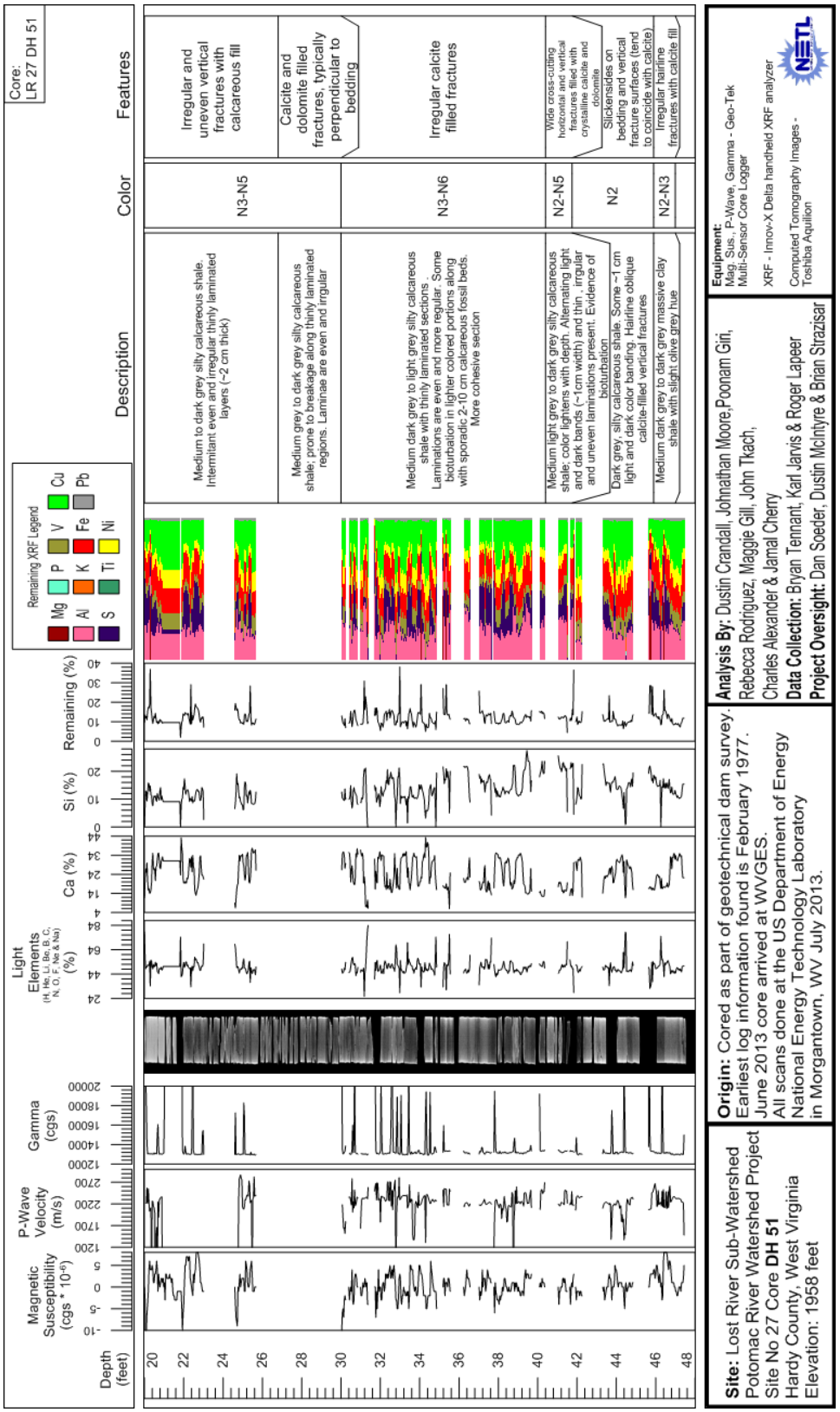

Figure 37: Combined core log for Lost River 27 Drill Hole #51.

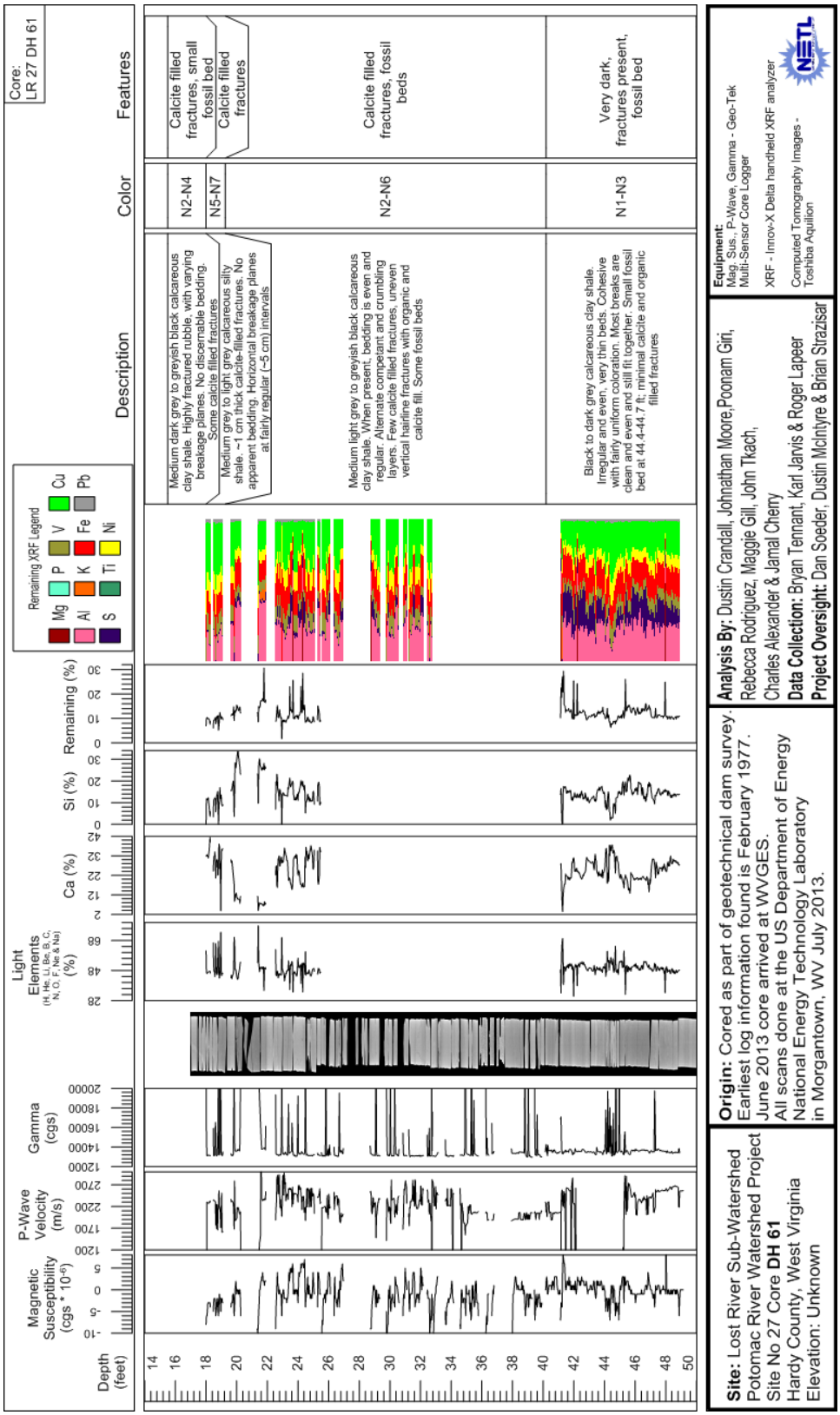

Figure 38: Combined core log for Lost River 27 Drill Hole #61.

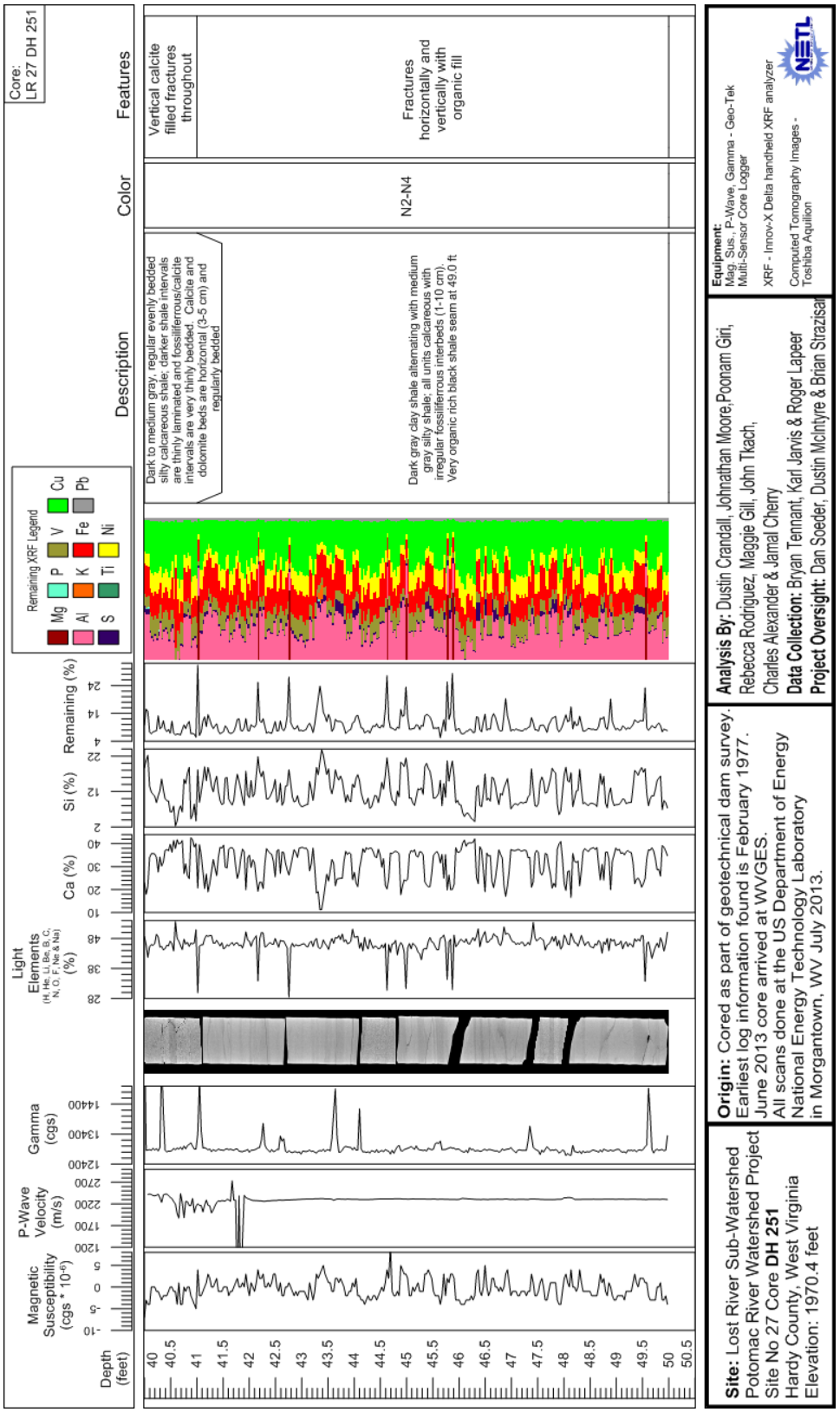

Figure 39: Combined core log for Lost River 27 Drill Hole #251.

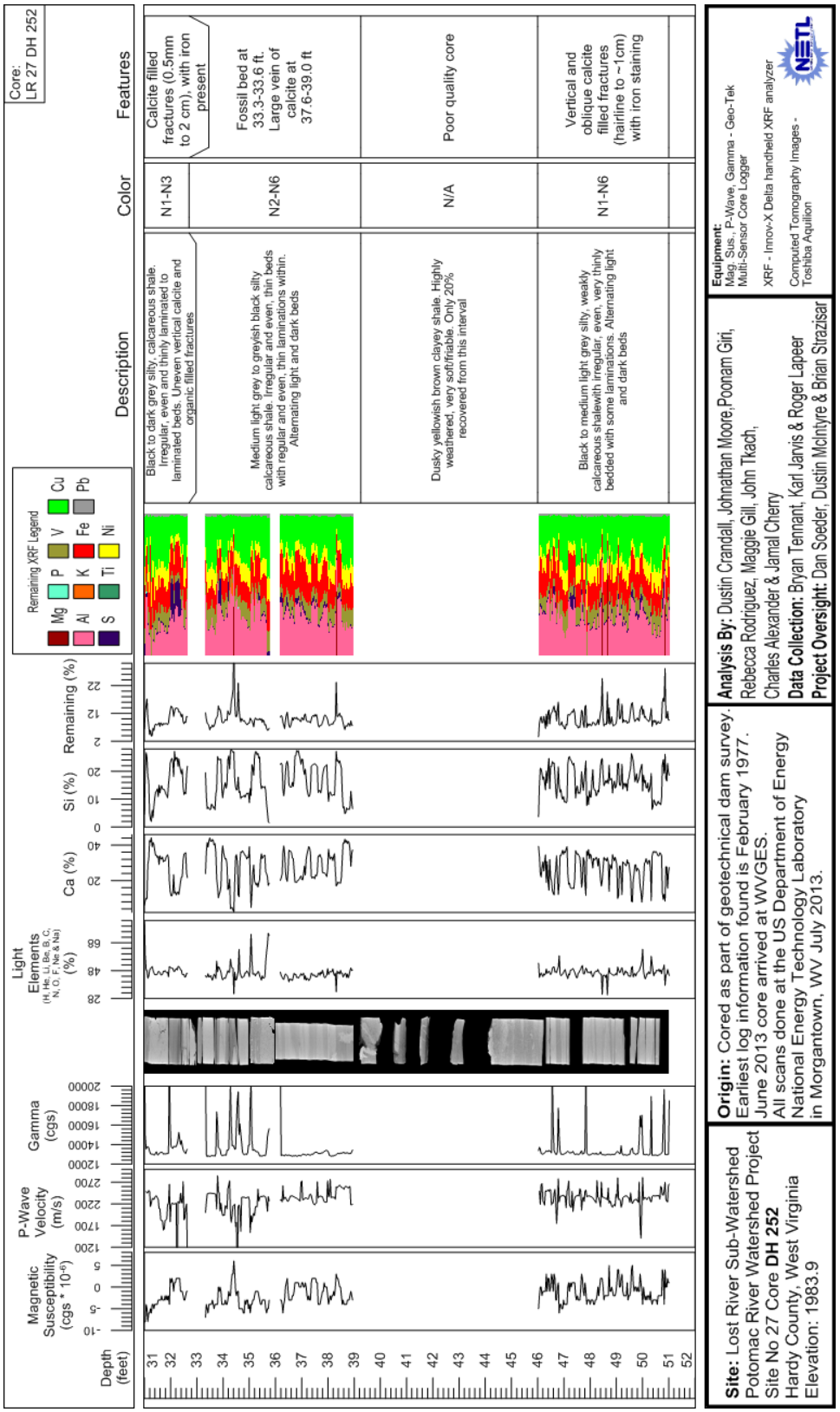

Figure 40: Combined core log for Lost River 27 Drill Hole #252.

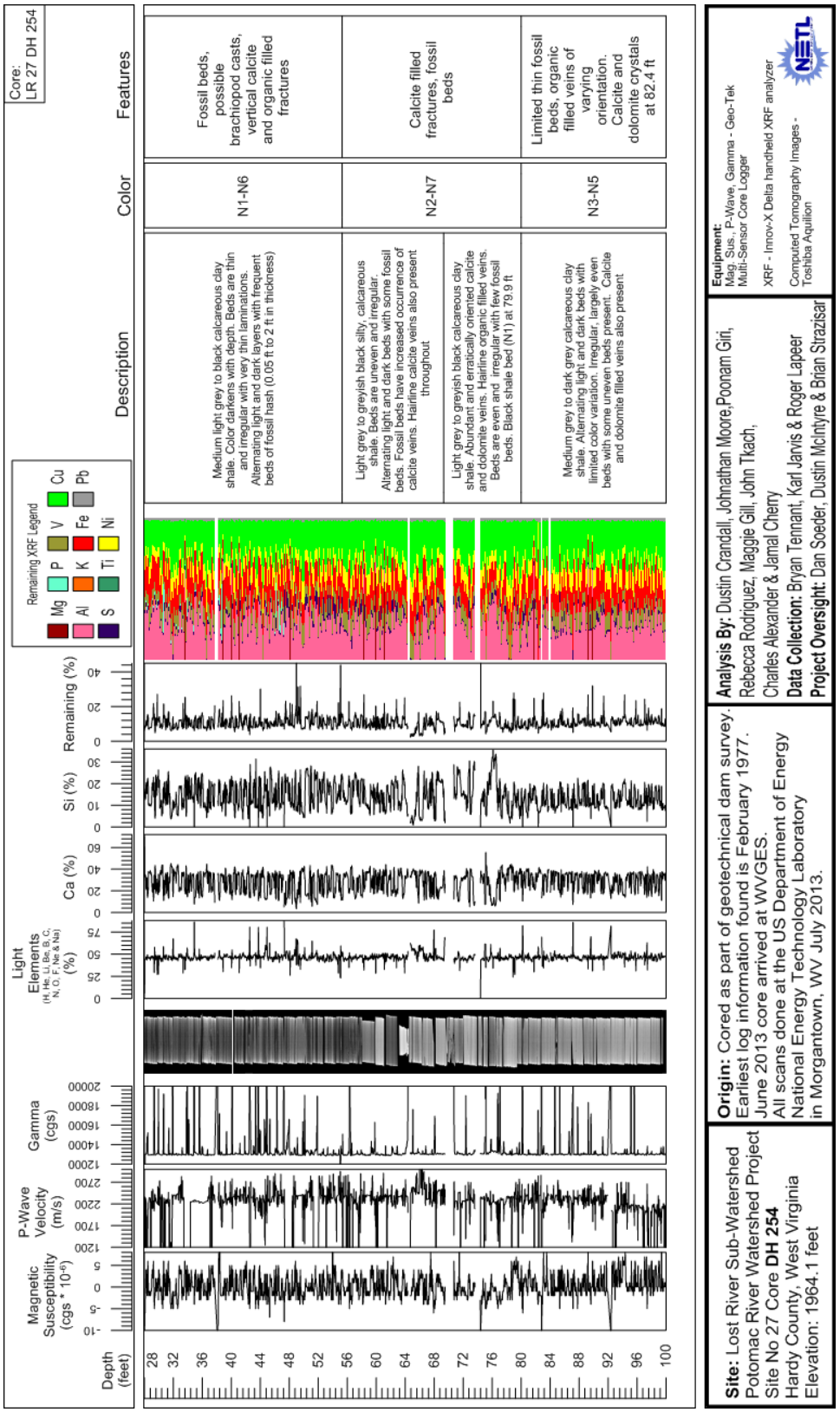

Figure 41: Combined core log for Lost River 27 Drill Hole #254.

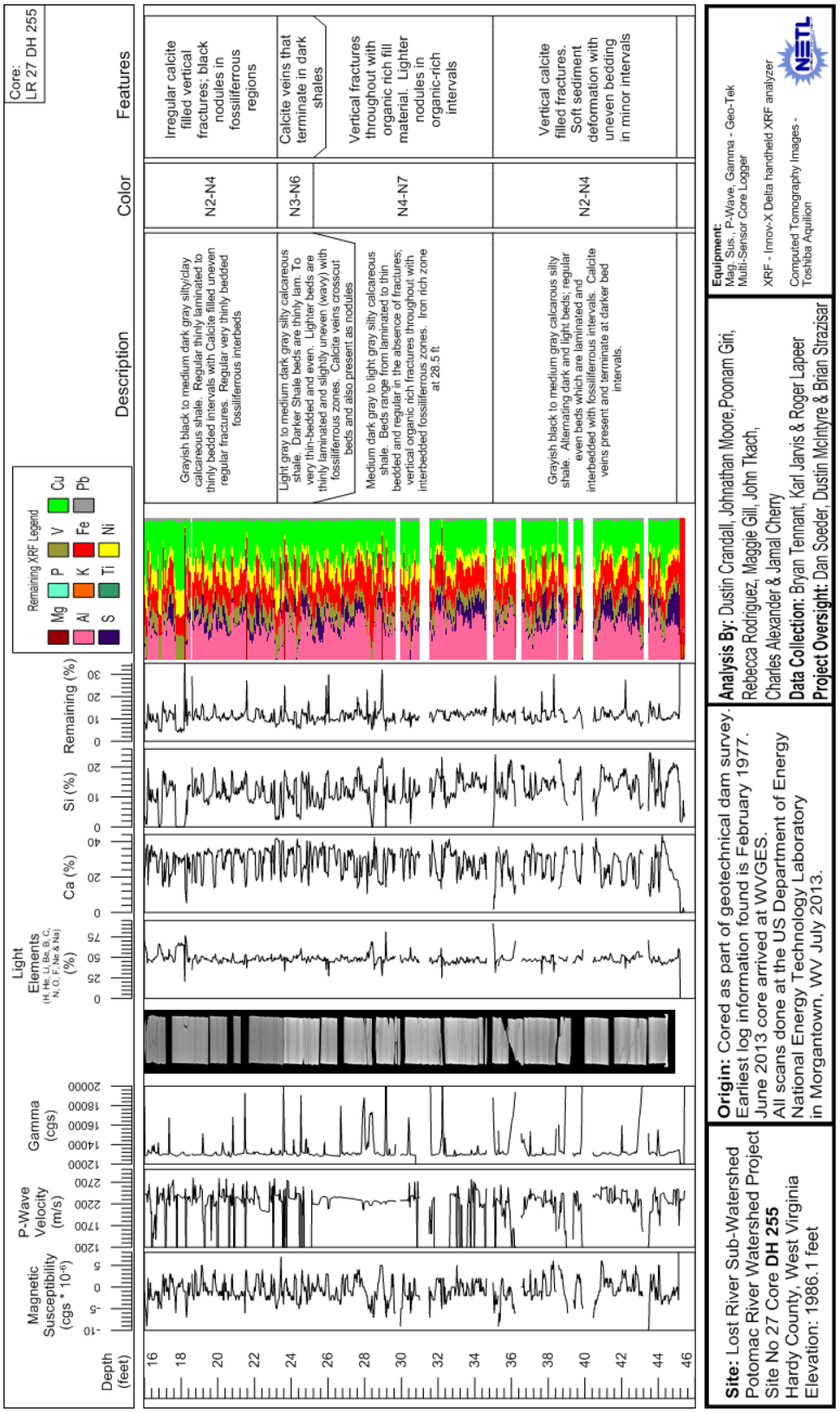

Figure 42: Combined core log for Lost River 27 Drill Hole #255.

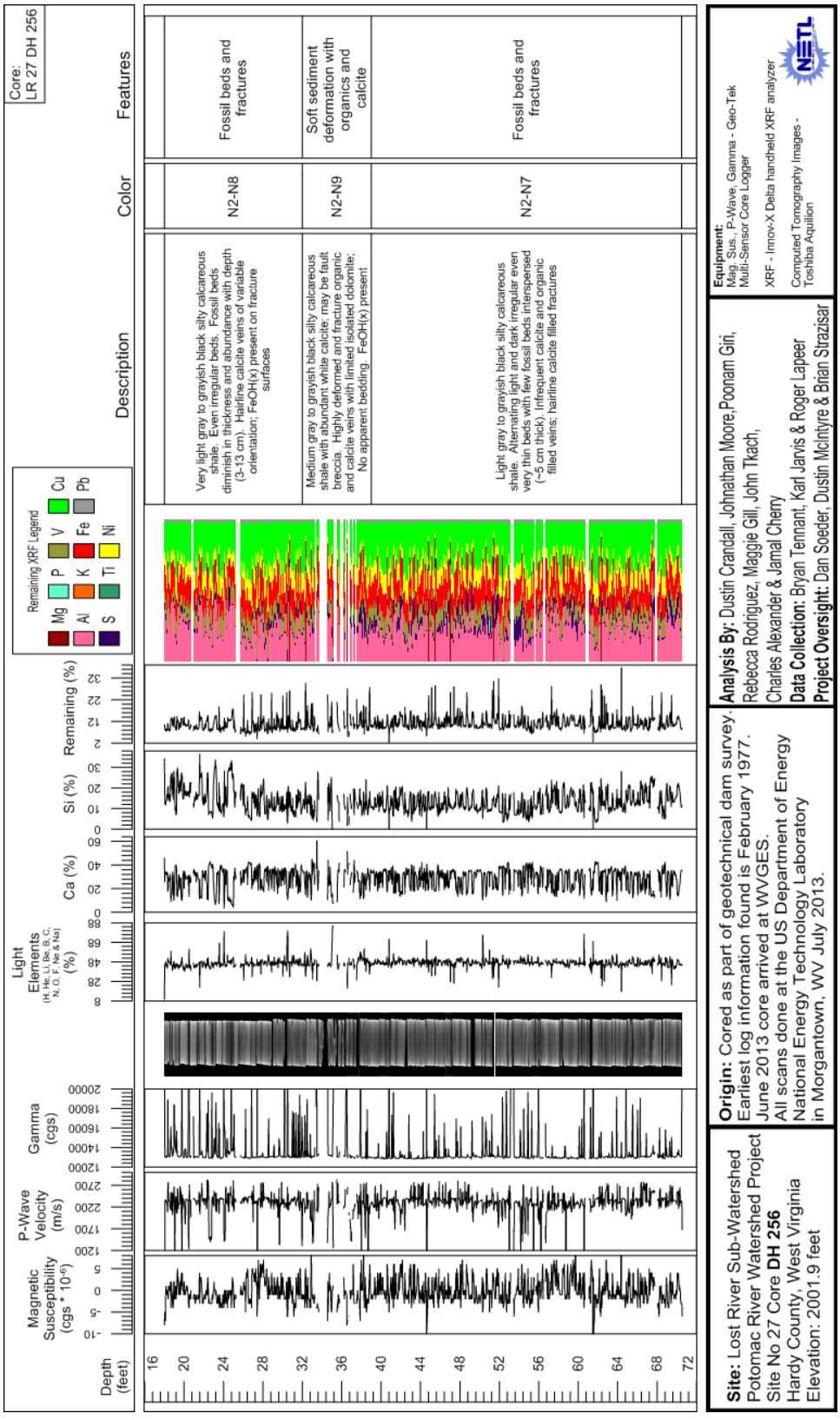

Figure 43: Combined core log for Lost River 27 Drill Hole #256.

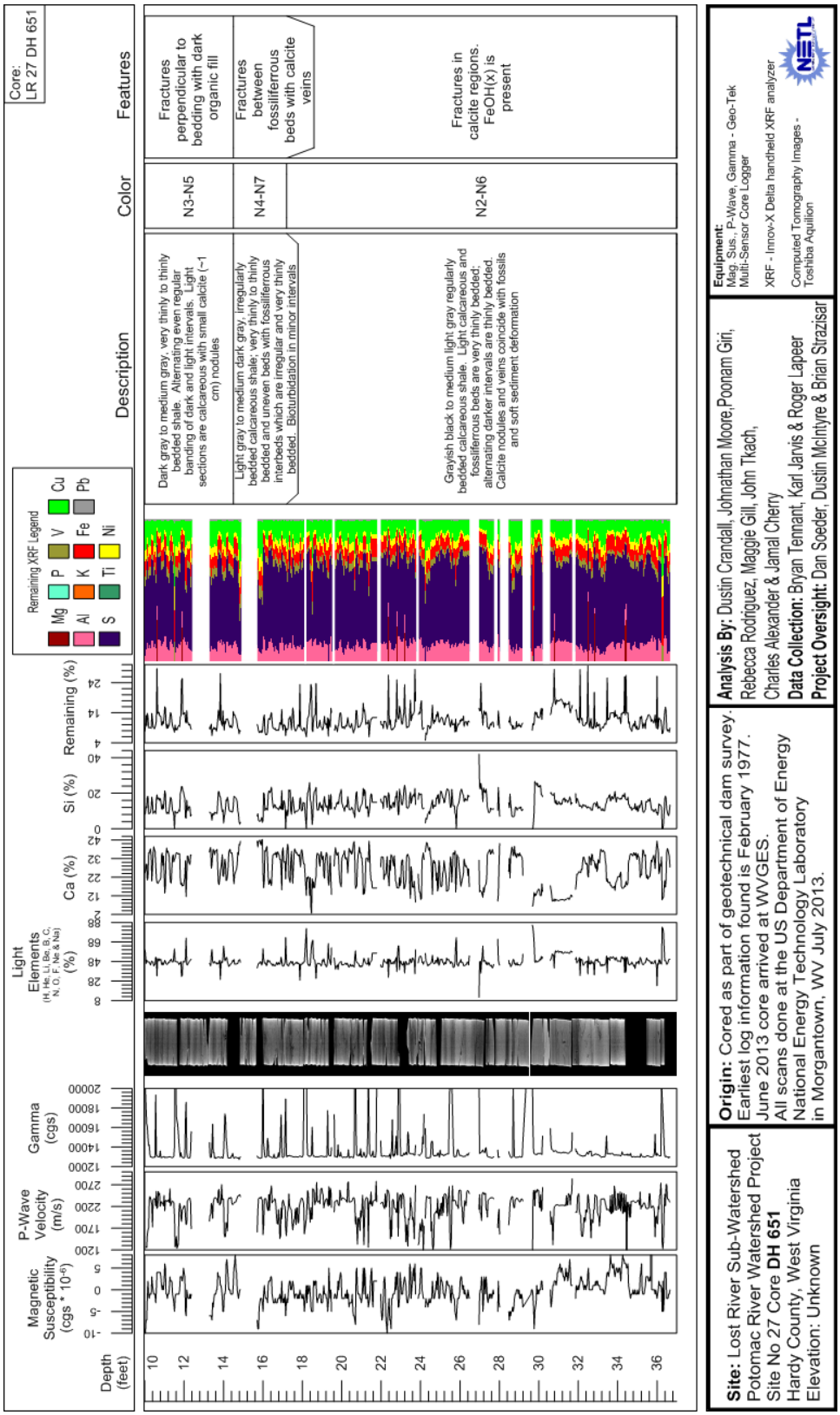

Figure 44: Combined core log for Lost River 27 Drill Hole #651.

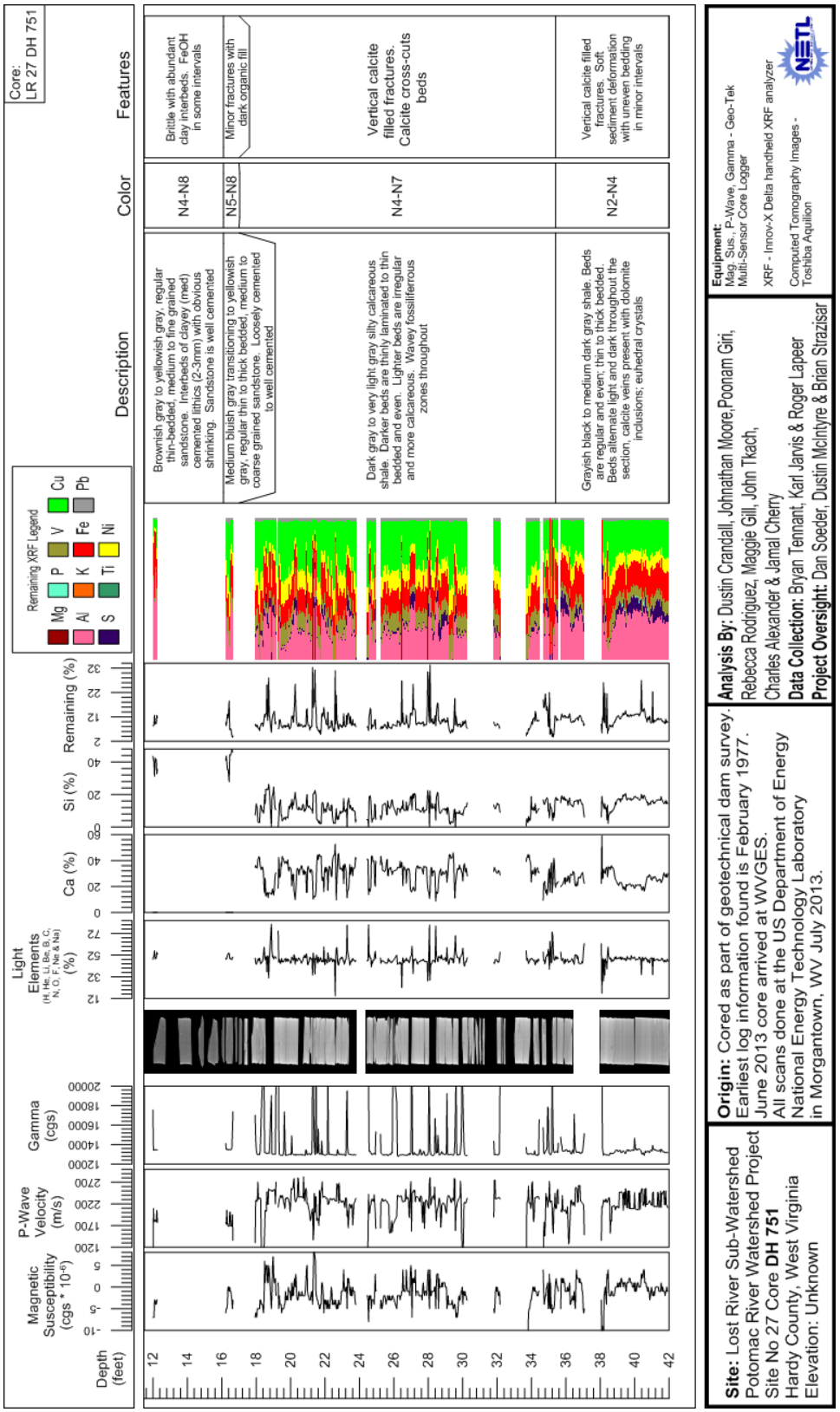

Figure 45: Combined core log for Lost River 27 Drill Hole #751.

4.1.3 Industrial CT scans

The industrial CT scans were conducted at varying resolutions based on the overall size of the sample. As mentioned previously, the grayscale ranges differ due to density variability within and between the samples, where the minimum and maximum grayscale values are dependent on the least and most dense materials. The grayscale values in the following images were used to isolate and visually differentiate objects of interest in the scans, such as fractures and organic-rich regions. Each image set is comprised of four different views of the same core at varying angles to fully display the features in 3D, and is accompanied by a photograph of the original core.

As explained in a previous section, the cores were spliced together by adjusting the grayscale histograms to match the highest and lowest values in each scan. This manipulation introduced some minor variability that can be seen as disjointed features and slight grayscale discontinuities. Overall, these minor interferences were not large enough to prevent zonal isolation of features and thus provide a good approximation of said features.

The features documented in these images provide a detailed analysis of the cores via industrial scanning. The feature selection was performed by the authors, and as such should be considered subjective to a degree. Furthermore, although inherent histogram values were used to isolate features, those features were later cropped and fine-tuned by the researcher.

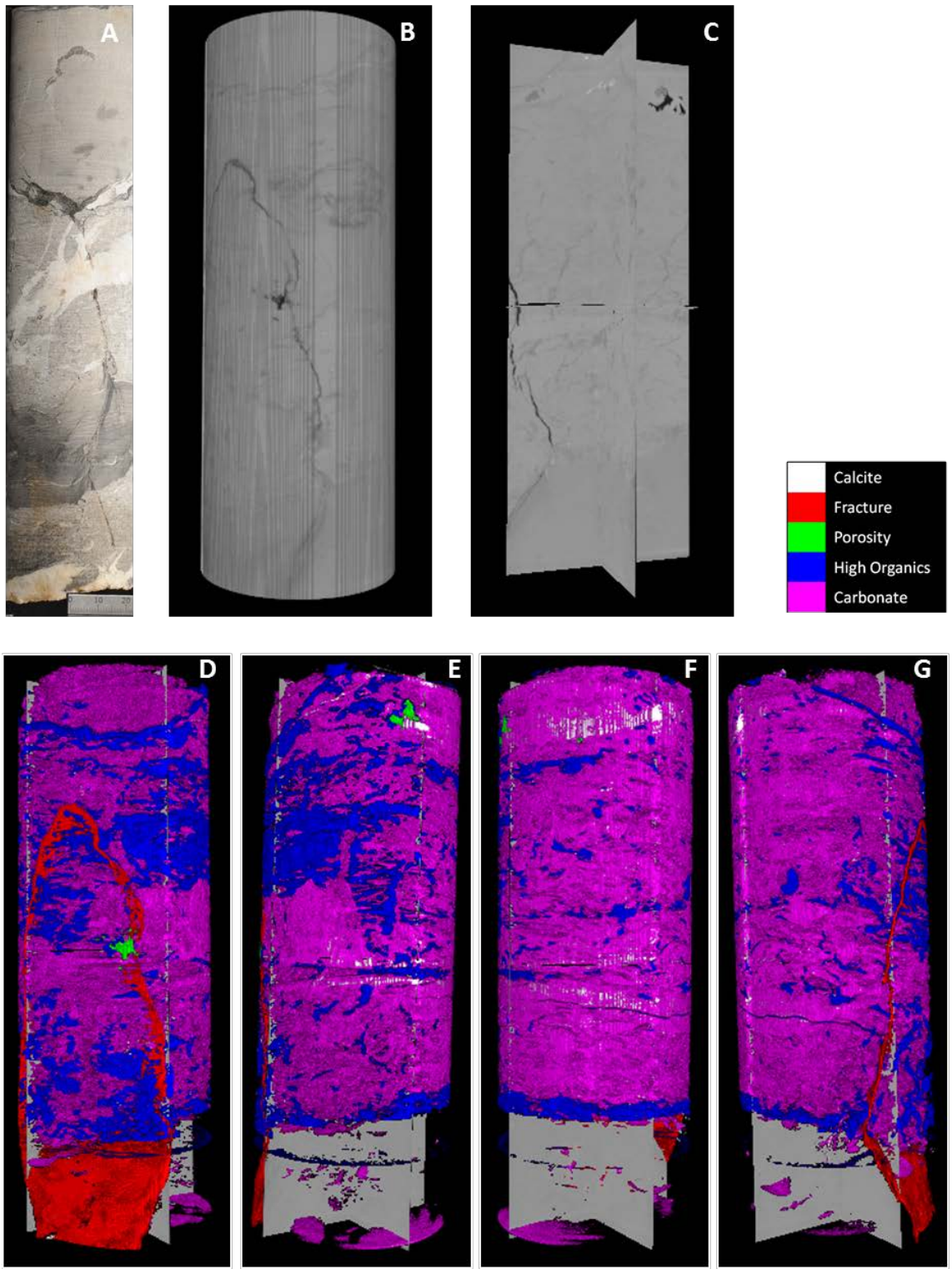

Figure 46: 3D representation of features from Lost River Drill Hole #251 at depth 40.2–41 feet. The images represent: A) original core (scale in mm), B) 3D volumetric scan, C) orthographic planes through the volume, D-G) respective 0, 90,180, and 270 degree rotations of volume with features outlined in designated color from the legend.

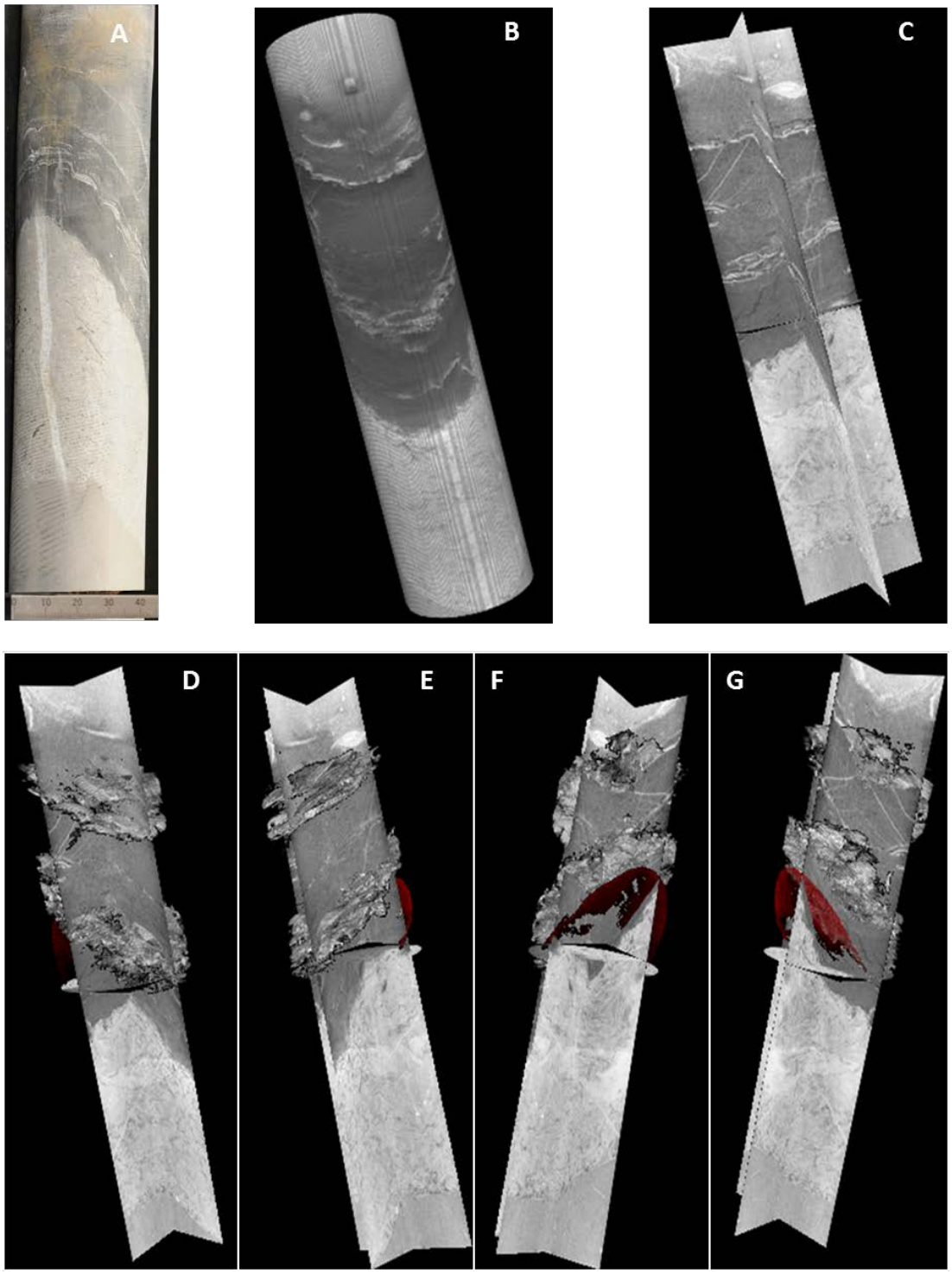

Figure 47: 3D representation of features from Lost River Drill Hole #254 at depth 72.9–73.5 feet. The images represent: A) original core (scale in mm), B) 3D volumetric scan, C) orthographic planes through the volume, D-G) respective 0, 90,180, and 270 degree rotations of volume with fossils (white) and fracture (red)

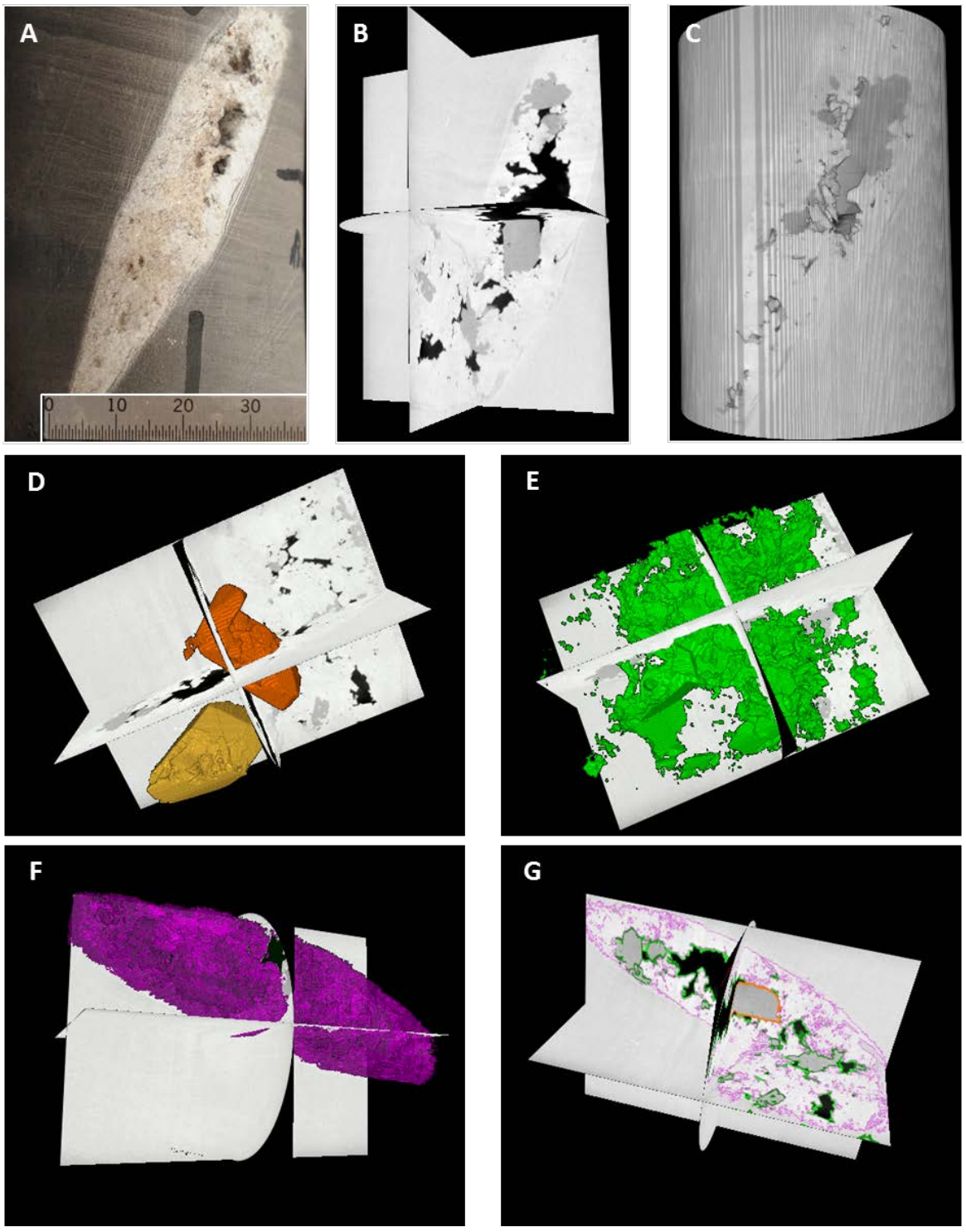

Figure 48: 3D representation of features from Lost River Drill Hole #751 at depth 36.0–36.4 feet. The images represent: A) original core (scale in mm), B) orthographic planes through the volume, C) 3D volumetric scan, D) calcite crystals (orange and yellow), E) porosity (green), F) carbonate (purple), and G) orthographic planes of full the scan with composite features outlined.

5. DISCUSSION

The incorporation of the MSCL, CT, and traditional sample analysis provided a multidisciplinary sample evaluation approach and allowed for a comprehensive and systematic sample analysis methodology to be developed. Use of these techniques in sample evaluation will allow for more consistent and robust data production at NETL.

By combining low resolution images from the medical CT scanning, the MSCL data, and traditional analysis techniques descriptions of hundreds of feet of core were developed with knowledge of both the internal structure and the macroscopic changes in lithology. These techniques are all non-destructive, rapid, and when performed in parallel give insight into the core make-up that is above and beyond what one individual technique can provide. These techniques can be used to identify zones of interest within larger cores for detailed analysis and quantification.

High resolution images from the industrial CT scanning allow for an impressive understanding of the internal structure of these cores without destroying the samples. But the large data size, and the significant time commitment required to scan and analyze these cores requires that samples be picked judiciously to maximize the research benefits from this analysis. As shown in Figures 47 ad 48, samples with fractures and discernable flow features can be scanned to obtained relevant flow feature characterizations. But samples, such the one shown in Figure 46, with little internal variation in structure result in limited benefits from the high resolution scanning technique. These results indicate for future analyses of core, where the most relevant sections for research analysis are not known *a priori*, that low resolution medical, traditional, and MSCL data is collected first to isolate zones of unique interest for the high resolution and detailed analysis that is available with the high resolution scanning techniques available at NETL.

This page intentionally left blank.

6. REFERENCES

Dunbar, C. O.; Rodgers, J. *Principles of Stratigraphy*; Wiley: New York, 1957.

Dyman, T. S. *Eastern Gas Shales Project (EGSP) Data Files: A Final Report*; U.S. Department of Interior Geological Survey Open-File Report 81-598, 1981. http://netl.doe.gov/kmd/cds/disk7/disk1/EGS%5CEastern%20Gas%20Shales%20Project%20%28EGSP%29%20Data%20Files%20A%20Final%20Report.pdf

Geotek Ltd. Geotek Multi-Sensor Core Logger Flyer, Daventry, UK, 2009. http://www.geotek.co.uk/sites/default/files/MSCLOverview.pdf

Geotek Ltd. Multi-Sensor Core Logger Manual; Version 05-10; Published by Geotek, 3 Faraday Close, Daventry, Northamptonshire NN11 8RD, 2010. info@geotek.co.uk, www.geotek.co.uk

Mckee, E. D.; Weir, G. W. Terminology for Stratification and Cross-Stratification in Sedimentary Rocks. *Geological Society of America Bulletin* **1953,** *64.4*, 381–90.

Pettijohn, F. J. *Sedimentary Rocks. Harperś Geoscience Series*, 2d Ed.; Harper: New York, 1957.

Rasband, W. S.; ImageJ. U.S. National Institutes of Health: Bethesda, MD, 1997–2016, http://imagej.nih.gov/ij/ (accessed 2017).

Ryder, R.T.; Crangle, D. C. *Stratigraphic Framework of Cambrian and Ordovician Rocks in the Central Appalachian Basin from Richland County, Ohio to Rockingham County, Virginia. Reston, VA*; U.S. Dept. of the Interior, U.S. Geological Survey, 2002.

This page intentionally left blank.

Sean Plasynski
Executive Director
Technology Development & Integration Center
National Energy Technology Laboratory
U.S. Department of Energy

Jared Ciferno
Associate Director
Oil and Gas
Technology Development & Integration Center
National Energy Technology Laboratory
U.S. Department of Energy

Elena Melchert
Director
Division of Upstream Oil and Gas Research
U.S. Department of Energy

Cynthia Powell
Executive Director
Research & Innovation Center
National Energy Technology Laboratory
U.S. Department of Energy

NETL Technical Report Series